

Manuscript for

J. Phys.: Condens. Matter 18(30), S1629-S1653 (2006).

Selective chemical bond breaking characteristically induced by resonant core excitation of ester compounds on a surface

Running head: Selective bond breaking by resonant core excitation

**Shin-ichi Wada, Hiroyuki Kizaki, Yoshihiro Matsumoto, Ryohei Sumii¹
and Kenichiro Tanaka**

Department of Physical Science, Hiroshima University, Kagamiyama,
Higashi-Hiroshima 739-8526, Japan

E-mail: swada@sci.hiroshima-u.ac.jp

¹ Present address: Research Center for Materials Science, Nagoya University, Furo-cho, Chikusa-ku, Nagoya 464-8602, Japan.

Abstract

Inner-shell excitation possesses an attractive potential to induce selective chemical bond breaking due to its special localization and atomic selectivity. This paper reviews our recent works about site-selective (or site-specific) photon stimulated desorption (PSD) of core-excited ester compounds, poly(methyl methacrylate) (PMMA) thin films, condensed methyl isobutyrate (MIB) multilayers, methyl ester terminated self-assembled monolayers (SAMs), partially deuterated SAMs and ethyl ester terminated SAMs. Exact selective bond breaking was observed for all molecular systems except for MIB multilayers: COO-R (R = CH₃, C₂H₅) breaking in the $\sigma^*(\text{COO-R}) \leftarrow \text{C } 1s, \text{O } 1s(\text{OR})$ excitations and CO-OR in the $\sigma^*(\text{CO-OR}) \leftarrow \text{O } 1s(\text{OR})$ excitation. Such resonant excitations take place within the functional group locally and the initial memory of the excited site and its localization character is effectively conserved during the PSD process even after subsequent Auger decays and ionic dissociation/desorption. Variation of selectivity observed here indicates the importance of the molecular environment and the contribution of the indirect dissociation process due to statistical energy relaxation and x-ray-induced electron stimulated desorption. The obvious polarization dependence measured only for selectively desorbing ions also supports the above characteristics. Neutral fragments desorbing from core-excited PMMA follow the profile of the total electron yield spectrum but not the partial ion yield of corresponding ions. This result indicates that ionic dissociation locally promoted by Coulomb repulsion plays an important role to reveal site-selectivity in chemical reactions induced by core-level excitation.

1. Introduction

Many experimental and theoretical studies in a soft x-ray region have been performed utilizing characteristics of inner-shell excitation. Spectroscopy in an energy domain such as x-ray absorption spectroscopy (XAS, NEXAFS), x-ray photoelectron spectroscopy (XPS) and Auger electron spectroscopy (AES) has been well established as a standard analytical technique in material science [1, 2]. Dissociation and desorption reactions of core-excited molecules have also been studied widely in isolated gaseous molecules, clusters, adsorbates, condensed molecules and polymers based on molecular spectroscopy, and various phenomena induced by inner-shell excitations have been investigated including decay dynamics of core-excited states and Auger final states. However, it is not yet established clearly how the characteristic nature of core-electron excitation is reflected in subsequent reaction dynamics.

Core excitation takes place within a quite local area, differently from valence excitation because of a special localization of the core electron, and its binding energy strongly depends on an element and its chemical environment, so a specific atom in a molecule can be excited selectively. Furthermore, as the core excitation is a transition process with an extremely high energy, the core-excited state decays within a quite short time period ($<10^{-14}$ s). In particular, in the case of light element atoms like second row elements, the Auger decay process, which is a non-radiative process, occurs dominantly around the excited atom, and commonly results in an electronically excited state with two holes (Auger final state). The Auger final state is also unstable and follows the ionic dissociation promoted by Coulomb repulsion between two holes, namely the Auger stimulated desorption (ASD) mechanism [3]. These consecutive decay processes suggest that the ionic dissociation initiated by the core excitation can conserve initial memory of a resonant excitation, namely from which inner-shell orbital to which antibonding orbital the excitation occurs locally, and therefore, if using a soft x-ray of tunable synchrotron radiation (SR), site-selective ionic bond breaking can be achievable in the vicinity of the excited atom. This is a quite unique phenomenon from the viewpoint of control of a chemical reaction: optically selective bond scission within a molecule, like a scalpel, which we term a ‘molecular scalpel’, as illustrated in figure 1 [4–6].

In this concept, site-selective (or site-specific) ionic fragmentation has been widely and successfully investigated in various core-excited molecular systems [7–28]² and [30–60] since the pioneer work by Eberhardt *et al* [4], although their finding for the site-specific ionic fragmentation of gaseous acetone has not been confirmed by later research [61, 62]. Baba emphasizes three general principles for realizing the highly specific chemical bond breaking by core-level excitation in his recent review article [8]. The first factor is that the photoexcitation at the K edge is more efficient than those at the L₁, L_{2,3} and M edges. Second, the element specificity clearly shows up with increasing difference in the atomic number of the two elements. Finally, if the resonant excitation from the core to valence unoccupied orbitals in a compound is a dipole-allowed transition, and the absorption-edge jump dramatically increases, this may result in highly specific fragmentation (resonance effect). On the basis of these speculations, he terms three kinds of specific dissociation/desorption patterns: ‘element-specific’ reaction (i) and ‘site-specific’ reactions due to a chemical shift (ii) and due to a resonant excitation to a specific unoccupied orbital (iii). The third resonance pattern is more effective for realizing selective chemical bond scission, even intuitively.

However, it should be noted that a serious question about the selectivity of the bond breaking still remains to be solved, since there is the possibility of losing the specific character of the core excitation through various competitive channels such as the delocalization of excess energy, especially in isolated gaseous molecules. In order to explain the difference in ionic dissociation reaction between that in the gas phase and at a surface, we proposed a hypothetical reaction scheme as shown in figure 2 [6, 48, 49]. The primary core excitation and the Auger decay are very fast processes of less than picosecond order, so it is considered that there are essentially no differences until an Auger final state between the gas phase

² Ultra-fast dissociation in core-excited states of gaseous molecules can also be classified into site-specific fragmentation. For example, see [29].

and the surface. Generally, Auger final states have large excess energies of 10–30 eV. On the basis of these facts, we assumed that there are two thermodynamic paths leading to ionic dissociation (fragmentation) reactions. One is the statistical reaction path in which the excess energy delocalizes and redistribution of this energy leads to a variety of chemical reactions. The probabilities of these reactions in this reaction path can be determined by statistical considerations, and the reactions lose the memory of the site of the primary excitation. The other is the non-statistical reaction path in which direct and site-selective (and also site-specific) reactions occur. In the case of isolated gaseous molecules, the excess energy that diffuses over the molecule can lead to statistical chemical reactions and such statistical reactions are dominant, thus the site-selective (non-statistical) reaction is hidden. On the other hand, in the case of solid surfaces, the excess energy that diffuses over the molecule rapidly flows into the solid or neighbouring molecules, thus it does not contribute to chemical reactions. As a result, statistical reactions are suppressed and site-selective reactions are emphasized at the solid surface. According to this hypothesis, site-selective reactions may well be more prominent at the surface than the gas phase.

Our first research presented by Tinone *et al* demonstrated obvious site-selective photon stimulated desorption (PSD) of ionic fragments occurring in a thin film of poly(methyl methacrylate) ($-\text{[CH}_2(\text{CH}_3)\text{CCOOCH}_3\text{]}_n-$, PMMA) [48]: CH_n^+ ($n = 0-3$) and OCH^+ ions desorb dominantly in specific resonant core excitations as a consequence of selective ionic dissociation of the methyl ester group. The investigation points out the importance of the primary excitation to the antibonding orbital for a specific bond to trigger off the selective ionic bond breaking. Subsequently, our studies have clarified the mechanism of site-selective ion desorption of PMMA in detail by using an Auger electron–photoion coincidence spectroscopy [50] and an *ab initio* MO calculation [51].

PMMA is a good prototype molecule, which demonstrates remarkable site-selectivity in PSD of ions, and such selective PSD occurs within the functional group (methyl ester group) of its side chain. From this point of view, it is important to take notice of a difference of environment or structure of the functional group in order to investigate a variation of site-selectivity in ionic PSD. So, our investigations were expanded to core excitations of a series of ester-group modified self-assembled monolayers (SAMs) and condensed multilayers of a pseudo-monomer molecule of PMMA. The SAM has attracted considerable interest as a well ordered organic monolayer which can be variously formed by substituting the end functional group [63, 64]. In particular, it is expected that the SAM has an advantage to improve site-selectivity in surface-sensitive ion desorption because the SAM can be prepared with highly oriented functional group on the topmost surface.

This paper reviews our recent works about site-selective PSD of core-excited ester compounds, which is organized as follows. The outline of the experimental methods and apparatus are described. Then the characteristic and mechanism of PSD are discussed based on ion desorption measurements in the C 1s and O 1s core excitations. The site-selective desorption reaction is inevitably disturbed by an accompanying indirect photodesorption process. Such direct and indirect processes are evaluated quantitatively. In the following section, results obtained for polarization-dependent measurements of ionic PSD are presented. Finally, photodesorption of neutral products is discussed.

2. Experimental details

2.1. NEXAFS and ionic PSD measurements

Measurements for near edge x-ray absorption fine structure (NEXAFS) and PSD of ions were carried out on the beamline BL7A [65] at the Photon Factory, High Energy Accelerator Research Organization (KEK-PF), and PSD measurement of neutral photoproducts was on the beamline BL13 at HiSOR of Hiroshima University. The experimental chamber had base pressure in the 10^{-9} Torr range for PMMA and SAM measurements at room temperature and 5×10^{-10} Torr for a condensed multilayer at 100 K. All measurements were performed with the spectral resolving power ($E/\Delta E$) of about 1500 and 700 in the C 1s and O 1s excitation regions, respectively. Photon energy was calibrated precisely by the intense σ^* resonance of highly oriented pyrolytic graphite (HOPG) [66] and the π^* and Rydberg states of gaseous CO_2 [67]. The π^* (C=O) resonances from C 1s(C=O) and O 1s(C=O) of PMMA were assigned to be at 288.4 and 532.3 eV, respectively, which are consistent with the reported values within the experimental error [68]. All spectra were corrected for fluctuations in SR light intensity and also normalized by intensities at pre-edge and ionization continuum after their backgrounds were subtracted. During the measurements, any irradiation damage of the samples was not confirmed.

Figure 3 shows the typical experimental set-up, where a usual time-of-flight mass spectrometer (TOF-MS) is introduced. Total electron yield (TEY) spectra, which are regarded as equivalent to absorption spectra, were obtained by measuring a sample drain current during x-ray irradiation. Total ion yield (TIY) spectra were obtained by non-mass-selected ions using TOF-MS. Partial ion yield (PIY) spectra for each photodesorbing ion were obtained from TOF spectra by changing photon energies. In this TOF measurement, we need a several hundred to thousand nanosecond time interval between photoirradiation (i.e. ion desorption) and ion detection as well as a pulsed signal of SR light or the other synchronized signal as a trigger. So, pulsed SR light in single bunch operation of the KEK-PF storage ring was utilized by taking a trigger of the 1/312 divided signal (624 ns interval) of the 500 MHz microwave cavity frequency [52]. In this case, the TOF spectrum is composed by superposition of the spectra triggered by several cycles of SR light. These NEXAFS and TOF measurements are essential experiments in this study. Details of the other experimental set-ups for the polarization-dependence measurement of ionic PSD and the measurement of neutral PSD are described in the following subsections.

2.2. Polarization-dependence measurement of ionic PSD

The polarization dependence can be measured by rotating a sample holder, while TOF-MS is generally installed in a chamber at a fixed direction. So, if the surface normal direction deviates from the TOF direction, the detection yield of desorbing ions falls rapidly. Therefore, it is required in this study to detect

desorbing ions suitably at each different incident angle. Some successful experiments for polarization-dependent PSD measurements have been reported by using a rotatable quadrupole mass spectrometer (QMS) [30] and a rotatable TOF-MS [36].

In our experiment, polarization-dependence measurements of photodesorbing ions were demonstrated using existing TOF devices and additional correction electrodes on both sides of the sample holder, as shown in figure 4, to rectify the trajectory of photodesorbing ions and make detection yield high enough in the off-normal arrangements between the sample and TOF-MS [53]. As there is a limit to the off-normal angle range measurable by the correction electrodes, two equivalent TOF devices are installed in the chamber at 30° and 70° from the incident SR (denoted by TOF60 and TOF20, respectively) to make measurements possible in wide incident angle range (10°–80°). TOF spectra at the incident angles from 10° to 40° were measured by TOF20 and those at 40°–80° were by TOF60.

2.3. Neutral PSD measurement

The experiment combining SR and lasers was performed on the soft x-ray beamline BL-13 at HiSOR [54]. A schematic description of the experimental set-up is illustrated in figure 5. A PMMA thin film was irradiated by SR light in the C 1s and O 1s excitation regions, which released neutral and ionic products. The photodesorbing neutrals can be ionized by a nonresonant multiphoton ionization (NRMPI) using an intense and ultrashort pulse laser. In this process, the desorbing neutral atoms and molecules can absorb multiple photons during a short period within a laser pulse and be ionized non-selectively and efficiently. The Ti:sapphire laser system (Spectra Physics) generated output light pulses of 800 nm with ~0.6 mJ pulse energy at 1 kHz repetition. In this experiment, the pulse width of the output light was expanded up to ~200 fs to obtain an efficient NRMPI signal. Laser light was introduced into the chamber through the lens near the sample substrate and focused a few millimetres away from the sample. The ionized neutral products were detected by TOF-MS selectively with the laser pulse as a trigger.

The TOF spectra measured by SR and laser irradiation consist of the desorbing neutral and ionic products and the components of residual gas in the chamber (case 'A'). Since desorbing ions do not correlate with each laser shot, they are easily removed from the TOF spectra as structureless background signals. On the other hand, the TOF spectra obtained only by laser irradiation correspond to the components of the residual gas (case 'B'). Thus, the net signals originating from the desorbing neutrals are obtained by subtracting 'B' from 'A'.

2.4. Chemicals

Chemicals used here are illustrated in figure 6. PMMA thin films were prepared by spin-casting from the methyl ethyl ketone solutions onto Au coated Si substrates, of which thicknesses were evaluated to be 200–500 Å. SAMs were prepared by immersing Au coated Si substrates into 1.0 mM ethanol solutions of methyl 16-mercaptohexadecanoate ($\text{HS}(\text{CH}_2)_{15}\text{COOCH}_3$, MHDA), its partial deuteride

(HS(CH₂)₁₅COOCD₃, MHDA-*d*₃) and ethyl 16-mercaptohexadecanoate (HS(CH₂)₁₅COOC₂H₅, EHDA) (NARD Institute Ltd) for 72 h. The methyl isobutyrate ((CH₃)₂CHCOOCH₃, MIB) molecule, which has the same structure as the monomer unit of PMMA, was also measured in a condensed multilayer condition cooled by liquid nitrogen. Although the molecular structures of chemicals are simply illustrated in the figure, the molecular orientation of PMMA as well as MIB is random in the film because the atactic PMMA is used in this study. On the other hand, SAMs form monolayers where the methylene chains are inclined by about 40° [69] and the end functional groups face the topmost surfaces. These differences in orientations are easily confirmed by measuring the polarization dependence of NEXAFS.

3. Ion desorption of core-excited ester compounds

3.1. NEXAFS spectra in C 1s excitation

Figure 7 shows NEXAFS spectra in TEY (upper) and TIY (middle) modes measured for (a) PMMA thin film, (b) condensed MIB, (c) MHDA SAM and (d) EHDA SAM in the C 1s core excitation [55]. Each spectral feature can be assigned as shown in the figures. The TEY spectra for PMMA and MIB resemble each other because spectral features are mainly attributed to the methyl ester group, while in the case of SAMs the spectra consist of the peaks of Rydberg transitions and broad σ^* resonances around 293 eV due to long methylene chains [70] as well as end functional groups. On the other hand, TIY spectra of PMMA and SAMs show characteristic structures around 289 eV, while that of MIB is similar to its TEY spectrum. This enhanced peak of PMMA is assigned to the transition to the $\sigma^*(\text{O}-\text{CH}_3)$ antibonding orbital at the methoxy group of the side chain ($\sigma^*(\text{O}-\text{CH}_3) \leftarrow \text{C } 1s(\text{OCH}_3)$), which contributes obscurely to the TEY spectrum, and this indicates that ions desorb efficiently by this resonant excitation. Such distinctive peaks clearly appear for SAMs and can be assigned to the same σ^* resonant transitions. These findings are confirmed by following TOF measurements. Note again that the TIY spectrum of condensed MIB, which also consists of the same absorption contribution due to the methyl ester group, does not show such enhancement of ion desorption but is identical with the TEY spectrum.

For further qualitative comparison between samples, ion desorption efficiency (IDE) spectra, which are obtained by dividing TIY by TEY, are also shown in the lower panels of figure 7. The IDE spectra of PMMA and SAMs display characteristic enhancements only at ~289 eV, which can be fitted by single Gauss curves. So, these enhancements of ion desorption are caused only by the single $\sigma^*(\text{O}-\text{CH}_3)$ resonant core excitations for PMMA and the MHDA SAM and the $\sigma^*(\text{O}-\text{C}_2\text{H}_5)$ excitation for the EHDA SAM, respectively. The enhancement of the MHDA SAM is about twice as large as that of PMMA. As the PMMA thin film was prepared by spin-casting of atactic PMMA polymer onto the Au coated Si substrate, the ester group of the side chain does not necessarily face the surface. On the other hand, the MHDA SAM orients its functional group onto the surface. Therefore, the SAM has an advantage to emit its ionic fragments directly. The enhancement of the EHDA SAM, however, is four times smaller than that

of MHDA. As mentioned below in detail, heavier $C_2H_m^+$ ($m = 1-5$) ions mainly desorb specifically from the ethyl ester end group of the EHDA SAM in this excitation instead of CH_n^+ ions for the MHDA SAM. It is considered that, although the site-specific ionic dissociation is induced by the σ^* resonant excitation even for the EHDA SAM, in the subsequent desorption process such heavier ions are easily neutralized and the yield of the ions becomes small. The IDE spectrum of MIB shows no significant enhancement. It is considered that an intermolecular interaction under the condensed phase loses the memory of the site of primary excitation and suppresses site-specific ion desorption. These findings indicate that molecular environment is an important factor to effectively enhance the site-selectivity.

3.2. Site-specific bond breaking in C 1s excitation

In order to investigate photodesorbing ionic species, TOF measurements were performed for the PMMA thin film and MHDA and EHDA SAMs which indicate site-specific desorption in the C 1s region, and the photon energy dependence of each ion (PIY spectrum) was investigated [55, 56]. Figure 8 shows typical TOF spectra measured at the $\sigma^*(O-CH_3, O-C_2H_5)$ resonances for PMMA, MHDA and EHDA. In the case of PMMA, H^+ , CH_n^+ and OCH^+ ions mainly originating from the side chain were measured, while additional ions originating from the methylene chain, $C_xH_y^+$ ($x = 2, 3$), were also measured for MHDA and EHDA SAMs as well as ions desorbing from end functional groups.

Typical PIY spectra of the photodesorbing ions from PMMA and the MHDA SAM are depicted in figures 9(a) and (b). In both cases, ion desorption has a strong dependence on the initial excitations and displays structural differences. In particular, it is clearly seen that CH_n^+ series uniquely desorb in the resonant excitation to the antibonding orbital mainly localizing at the $O-CH_3$ bond, $\sigma^*(O-CH_3) \leftarrow C\ 1s(OCH_3)$, at 288.9 eV. On the other hand, PIY profiles of the ions directly desorbing from the moieties where core excitation does not directly take place, like OCH^+ for PMMA and $C_2H_3^+$ and $C_2H_5^+$ (or OCH^+) for MHDA, mostly correspond to their NEXAFS structures in TEY. Such ions only desorb in proportion to absorption intensity. This specificity of desorbing ions really indicates a characteristic of resonant core excitation induced site-selective bond breaking: resonant excitation makes a bonding power weakened by pumping a core electron into its antibonding orbital and consequently promotes ionic dissociation.

H^+ ions desorb in large number and also show enhancement of the yields in the $\sigma^*(O-CH_3)$ resonance, which is seen as a blueshifted (or shoulder) peak of the main π^* resonance peak. In order to make this clear, the deuteride of MHDA in the methoxy group of the end functional group, MHDA- d_3 , was measured, and representative PIY spectra of the photodesorbing ions are shown in figure 9(c). It is clearly seen that the PIY spectrum of the H^+ ion desorbing from the methylene chain resembles the TEY spectrum, while that of the D^+ ion originating from the methoxy group shows the characteristic feature at the $\sigma^*(O-CD_3)$ excitation as the same as CD_n^+ . This result indicates that the resonant excitation of a C 1s electron in the methoxy group to the adjacent $O-C$ antibonding orbital takes place only within the functional group, and even after subsequent Auger decay and ionic dissociation/desorption, the initial memory of the excited site and its localization character is effectively conserved during the PSD process.

It should be emphasized that this is a straightforward example that the characteristic of core excitation is reflected in reaction dynamics directly.

In the PSD of EHDA depicted in figure 9(d), various photodesorbing ions were observed, like H^+ , CH_n^+ , C_2H_m^+ , OCH^+ and OC_2H_m^+ ions. In particular, C_2H_m^+ ions desorb site-specifically in the $\sigma^*(\text{O}-\text{C}_2\text{H}_5)$ excitation, while PIYs of H^+ and CH_3^+ are similar to the TEY spectrum. Relative yields of C_2H_m^+ ions with respect to H^+ become smaller in EHDA than that of CH_n^+ ions in MHDA. This reduction is due to suppression of the C_2H_m^+ ion desorption caused by neutralization during desorption. So, the enhancement of the site-specific PSD is apparently reduced in the IDE spectrum of EHDA. Precise quantitative detection of desorbing neutral species is indispensable to clarify the full picture of the PSD mechanism.

3.3. Site-selective bond breaking in O 1s excitation

Characteristic site-selectivity in PSD of a resonant core excitation is more obviously observed in the O 1s region [57]. Figure 10 summarizes the results obtained for (a) PMMA and (b) the MHDA- d_3 SAM. The top spectra are TEYs for both compounds, which display quite similar structure naturally in the O 1s excitation. As easily seen in the PIY spectra for both compounds, the CH_n^+ (CD_n^+) ions selectively desorb at 536.4 eV and desorption of the OCH^+ (OCD^+) ion is enhanced at 540.3 eV. The resonant state at 536.4 eV can be assigned to the excitation of the O 1s electron of the ether group to the antibonding orbital for the methoxy group ($\sigma^*(\text{O}-\text{CH}_3) \leftarrow \text{O } 1s(\text{COCH}_3)$) and hence ionic elimination of the methyl group is promoted. Similarly, the $\sigma^*(\text{C}-\text{OCH}_3) \leftarrow \text{O } 1s(\text{COCH}_3)$ transition at 540.3 eV causes ion desorption of the methoxy group selectively, which thereafter results in exothermic fragmentation to the OCH^+ ion ($\text{OCH}_3^+ \rightarrow \text{OCH}^+ + \text{H}_2$) [71]. This finding suggests that one can cut a different chemical bond efficiently and selectively by choosing proper irradiating soft x-ray energy with only a few eV energy difference. Moreover, site-selectivity of desorption in the MHDA(- d_3) SAM becomes far improved in comparison with that in the PMMA thin film in the O 1s region as well as C 1s region: this is easily seen by a comparison between profiles of the CH_3^+ or OCH^+ ion.

In the case of the EHDA SAM shown in figure 10(c), various photodesorbing ions were observed in the O 1s region as well. These PSDs can be classified into two site-selective dissociation/desorption patterns: C_2H_m^+ ions in the $\sigma^*(\text{O}-\text{C}_2\text{H}_5) \leftarrow \text{O } 1s(\text{COC}_2\text{H}_5)$ excitation and CH_n^+ , OCH^+ and OC_2H_m^+ ions (and also some H^+) in the $\sigma^*(\text{C}-\text{OC}_2\text{H}_5) \leftarrow \text{O } 1s(\text{COC}_2\text{H}_5)$ excitation, respectively. The PIY spectrum of mass 29 displays enhanced desorption in both the $\sigma^*(\text{O}-\text{C}_2\text{H}_5)$ and $\sigma^*(\text{C}-\text{OC}_2\text{H}_5)$ excitations. In this manner of classification, one can deduce that the main products in $\sigma^*(\text{O}-\text{C}_2\text{H}_5)$ and $\sigma^*(\text{C}-\text{OC}_2\text{H}_5)$ are C_2H_5^+ and OCH^+ ions, respectively. The PSD of CH_n^+ , OCH^+ and OC_2H_m^+ ions in the $\sigma^*(\text{C}-\text{OC}_2\text{H}_5)$ excitation can be explained by varied fragmentation processes of the $\text{OC}_2\text{H}_5^{+*}$ ion just after desorption: $\text{CH}_3^+ + \text{H}_2\text{CO}$, $\text{OCH}^+ + \text{CH}_4$ and $\text{OC}_2\text{H}_3^+ + \text{H}_2$ as exothermic reactions [57]. Similar consideration can be applied to the D^+ PSD for MHDA- d_3 SAM. D^+ from the methoxy group shows enhancement not in the $\sigma^*(\text{O}-\text{CD}_3)$ excitation but in the $\sigma^*(\text{C}-\text{OCD}_3)$ as well as OCD^+ . This result suggests that in the $\sigma^*(\text{O}-\text{CD}_3)$ excitation only neutral hydrogen elimination occurs after CD_3^{+*}

desorption, while OCD_3^{+*} ion desorbs selectively in the $\sigma^*(\text{C-OCD}_3)$ excitation with enough excess energy to lead to the endothermic proton elimination reaction, $\text{D}^+ + \text{D}_2\text{CO}$.

Besides a plausible explanation for the fragmentation of directly desorbing initial ions, R^{+*} and OR^{+*} ($\text{R} = \text{CH}_3, \text{C}_2\text{H}_5$), we should mention another experimental approach to explain production of variety of ions. In the ASD model, Auger final state is directly related to the ion desorption by core excitation. Auger electron-photoion coincidence (AEPICO) spectroscopy is useful for clarifying the relationship between the Auger final state and the ion desorption [9]. We have applied AEPICO measurements to the PMMA thin film [50] and the MHDA SAM [58], and proposed that the ion desorption is enhanced at the specific Auger final states related to spectator-type Auger decays where one excited electron remains in the antibonding orbital and two electrons are removed from bonding orbitals for the same chemical bonds (two hole-one electron states). For instance, in the $\sigma^*(\text{O-CH}_3) \leftarrow \text{C } 1\text{s}(\text{OCH}_3)$ transitions for both PMMA and MHDA, CH_3^+ and CH_2^+ (or CH^+) desorption show enhancements at two different Auger final energies: CH_2^+ and CH^+ ions are effectively produced at the Auger final states with about 5 eV higher internal energy than the state where pronounced production of the CH_3^+ ion occurs. This energy difference in the internal energy corresponds with the endothermic energy of a hydrogen atom or a hydrogen molecule elimination from the CH_3^+ ion (5.4 eV) [72]. Auger final states produce the highly vibrationally excited states of parent CH_3^+ fragment directly or possibly via internal conversion from different electronically excited states just after desorption, and then it dissociates into daughter fragments of CH_2^+ and CH^+ ions. The resonant core excitations to the $\sigma^*(\text{CO-R})$ and $\sigma^*(\text{C-OR})$ antibonding orbitals exactly cut their CO-R and C-OR chemical bonds, respectively.

We should also note that on careful comparison of the PSD of ions induced by C 1s and O 1s core excitations (figures 9 and 10), the fragmentation patterns of CH_n^+ and C_2H_m^+ ions in PMMA and SAMs show different behaviour, namely $\text{CH}^+/\text{CH}_3^+$ and $\text{C}_2\text{H}_2^+/\text{C}_2\text{H}_4^+$ ratios are higher in the $\sigma^*(\text{O-R}) \leftarrow \text{C } 1\text{s}(\text{OR})$ excitations than those in the $\sigma^*(\text{O-R}) \leftarrow \text{O } 1\text{s}(\text{OR})$ excitations, in spite of the resonant excitations to the same unoccupied antibonding orbitals mainly localizing at the O-R bonding. The subsequent fragmentation reaction of the removing R^+ group proceeds efficiently in the C 1s core excitation, but inefficiently in the O 1s excitation. Moreover, site-specificity becomes higher for H atom eliminated fragments in the C 1s excitation, while in the O 1s excitation there is no drastic change. In this case the only difference is that the core-excited atom is included in the removing R^+ group in the C 1s excitation, but not in the O 1s excitation. Thus we tentatively explain this finding as follows. In the C 1s core excitation the Auger final energy is concentrated within the desorbing R^+ group and used effectively for further fragmentation of R^+ , but in the O 1s excitation the Auger final energy easily diffuses into a remaining part on the surface and is not effectively used for the fragmentation.

Based on the above results, it should be emphasized that these two different types of fragmentation path can be classified into the following two types [59]. One is a bond scission accompanied by further fragmentation (named ‘hard-cut’). The other is a bond scission accompanied by less fragmentation (named ‘soft-cut’). These findings are important not only to elucidate the mechanism of

the selective chemical bond scission but also to apply this technique to the future controlling of chemical reactions.

4. Quantitative evaluation of direct and indirect dissociation

We have demonstrated that core-electron excitation can induce site-selective bond breaking in ester compounds on surfaces. However, not all of the photodesorbing ions necessarily reflect the selectivity. There are the following two important factors to disturb this characteristic phenomenon directly induced by core excitation. The core-excited state produced by soft x-ray irradiation immediately decays to an Auger final state, which is also a highly excited state (an excited state of a singly charged ion for the usual resonant Auger decay). So, it may be expected that fast inter- and/or intra-energy relaxation easily occurs in the final state. Such a statistical energy delocalization process can give rise to ionic dissociation at every possible site in a molecule, and as a result any ion desorbs with moderate yield not influenced by the nature of the excited state but only in proportion to the x-ray absorption intensity. The second factor is the x-ray-induced electron-stimulated desorption (XESD) process [33, 73]. After a photoabsorption of soft x-rays, Auger and inelastically scattered electrons are emitted not only from the surface but also from the bulk. Such energetic electrons can induce electronic transition accompanied by bond dissociation. In particular, ionic fragments created on a surface can easily desorb as they are. Such indirect processes also occur at every possible site in a molecule and lose the initial memory of the atom and bonding selectivity by a resonant core excitation.

Consequently, in many cases, these indirect processes make the ion yield signal simply a replica of the TEY spectrum originating from the bulk. In fact, the ion desorption via the indirect processes is a dominant process and its yield is often superior to the yield by the direct process, especially for a condensed multilayer molecule [73] as shown in figure 7(b) of MIB. The mixing of the direct and indirect processes make information on direct ion desorption phenomena obscure. In this section, direct and indirect processes are discussed quantitatively from PIY results for PMMA and SAMs in the C 1s excitation (figure 9) [56], as it may be considered that the component ratio between two processes derived from an ion yield spectrum consists of complex factors including not only the localization character during core excitation and subsequent reaction but also effects of inter- and intra-molecular environments [33, 73].

If the yield of a desorbing ion produced by the indirect process is in proportion to an absorption cross section as mentioned above, the ion yield spectrum may be considered to be the same as the TEY spectrum. On the other hand, a site-specific desorption via the direct process should occur only at a specific resonant state, like the almost 100% site-specific PSD of CH^+ and CD^+ ions in figure 9. So, the direct and indirect processes can be evaluated by the way in which the measured PIY spectrum is reproduced by the superposition of the moderately weighted TEY and the PIY of CH^+ (CD^+). Figure 11(a) depicts an example of spectral fitting of the TEY spectrum obtained for a C 1s-excited MHDA SAM. The

slash-marked area corresponds to the absorption component of the focused $\sigma^*(\text{O}-\text{CH}_3) \leftarrow \text{C } 1s(\text{OCH}_3)$ transition.

Analytical results for CH_3^+ PIY spectra of PMMA and MHDA are shown in figures 11(b) and (c), respectively. The thick lines describe the composed curves to reproduce the PIYs (\circ) by the TEYs (dotted (red) lines) and PIYs of CH^+ (solid (blue) lines). The reproduced curves coincide well with the PIYs, especially in the case of PMMA, which indicates that this analytical procedure is available to qualitative evaluation. The extracted components of the $\sigma^*(\text{O}-\text{CH}_3)$ excitations for the CH^+ PIYs (light grey (sky-blue) areas) and TEYs (dark grey (red) areas) correspond to the direct site-specific and indirect ionic dissociation processes, respectively. In CH_3^+ ion desorption of PMMA, the direct process in this resonance is estimated to be 65% and the indirect process is 35%. From good agreement between the measured PIY spectrum and the reproduced curve, it is considered that the majority of ion desorption is caused by the indirect process over the other excitation and ionization region. In the case of MHDA, the direct process of 90–95% and the indirect process of 5–10% are derived for the CH_3^+ desorption in the $\sigma^*(\text{O}-\text{CH}_3)$ excitation in the same manner, evaluating the improvement of specificity for SAM numerically. C_2H_3^+ ion desorption from EHDA is also shown in figure 11(d) as a typical result. The direct component in the $\sigma^*(\text{O}-\text{C}_2\text{H}_5)$ excitation was derived to be 85–90%, which is also higher than that of CH_3^+ for PMMA. The contribution of two dissociation processes, the direct (site-selective or site-specific) and indirect processes, to ion desorption could be elucidated for core-excited polymer film and SAMs. We must emphasize that MHDA and EHDA are monolayers and the $\sigma^*(\text{O}-\text{CH}_3, \text{O}-\text{C}_2\text{H}_5)$ resonant excitations take place within the end functional groups aligned onto the topmost surfaces, thus XESD process can be strongly reduced. The small contribution of the indirect desorption measured for CH_3^+ and C_2H_3^+ of SAMs in these resonances would be mainly caused by a statistical energy delocalization.

It should be noted here that the reproduced curves deviate from the PIY spectra with increasing photon energy. This is also confirmed in the IDE spectra of figure 7 for all samples as an increase of IDE intensities in the higher energy region. This phenomenon would be due to enhancement of ionic dissociation, since the kinetic energy of the photoelectron becomes higher and also multielectron excitation like shake-up and shake-off processes can take place above ionization potentials (>290 eV).

5. Polarization dependence of ion desorption

Thiol molecules which constitute an SAM adsorb on a substrate nearly upright through van der Waals interaction between the methylene chains so that their end functional groups are oriented densely on the topmost surface. Accordingly, the TEY spectrum of the SAM shows a clear incident angle dependence of the SR. In this respect, the polarization dependence of each ionic PSD in the C 1s and O 1s core excitations of the methyl ester-terminated SAM was measured to investigate whether the polarization dependence is conserved even in the succeeding ion desorption phenomena and what information about the reaction dynamics can be derived from the dependence [55, 60, 53].

Figure 12 summarizes the results of the polarization-dependent PSD measured in the C 1s excitation of MHDA- d_3 . An incident angle θ is given from the sample surface, which corresponds to an angle of the electric field vector from the surface normal. As shown in figures 12(a) and (b) respectively, intensities of CD_3^+ and D^+ ions obviously depend on the incident angle of SR in the $\sigma^*(O-CD_3) \leftarrow C\ 1s(OCD_3)$ excitation which induces site-specific PSD and show no change in the other excitations. On the other hand, H^+ desorption with no specificity is independent of the angle in the whole excitation region as shown in figure 12(c). Net intensities of these desorbing ions in the $\sigma^*(O-CD_3)$ excitation are plotted in figure 12(e) as a function of the incident angle θ . It is clearly seen that the site-specific PSD of D^+ , CD_2^+ , and CD_3^+ ions from the end functional group in the resonant excitation is enhanced at the grazing incident angle, while the desorption of H^+ shows almost flat dependence.

At grazing incidence of SR, the electronic field vector becomes parallel to the surface normal. Although the molecular structure of the MHDA (MHDA- d_3) SAM has not been investigated in detail, the bond axis of O-CH₃ lies very nearly along the surface normal ($\sim 14^\circ$ off) [69]. The grazing incident irradiation causes an enlargement of the $\sigma^*(O-CD_3)$ transition probability and consequently can enhance the specific PSD, since the electric field vector becomes close to parallel to the transition dipole moment nearly along the O-CD₃ axis. The dependence of these ions in other excitations is weak and such independence is also measured in the non-specific $C_2H_5^+$ and OCD^+ ion desorption. Only ions which display the site-specific PSD indicate a distinct polarization dependence clearly. This result also suggests that site-selective PSD takes place only within the functional group where the core electron is excited and the initial memory of the localization character of the core excitation is effectively conserved during subsequent Auger decay and ionic dissociation/desorption. On the other hand, ions which do not indicate the site-specific PSD like the H^+ ion, and even D^+ and CD_3^+ ions in the $\sigma^*(C-C)$ excitation, are not affected by the polarization of SR so much. It is considered that such different dependence is due to the dissociation mechanisms characterized as the direct and indirect dissociation. The former may conserve the polarization dependence of absorption and the latter is considered not to reflect the dependence because of randomization of the initial memory.

Trends of the dependence depicted in figure 12(d) become higher in the order CD^+ (not drawn in the figure), CD_2^+ , CD_3^+ and D^+ . This tendency is in good agreement with that of the specificity in the $\sigma^*(O-CD^3)$ desorption shown in figure 9(c). Considering that even CD^+ and CD_2^+ ions originating from the fragmentation of CD_3^+ have high desorption yields in the $\sigma^*(O-CD_3) \leftarrow C\ 1s(OCD_3)$ excitation compared with those produced in the corresponding O 1s excitation ($\sigma^*(O-CD_3) \leftarrow O\ 1s(OCD_3)$), see figure 10(b)), it can be concluded that such D atom eliminated fragments in the C 1s region are dominantly produced via the direct process where high enough excess energy is conserved locally around the excited atom in the removing CD_3 moiety, thus CD^+ and CD_2^+ are produced with high site-specificity and obvious polarization dependence. In the case of D^+ , as the desorption needs not only fragmentation but also charge transfer, the contribution of the indirect process becomes large in the PSD and D^+ displays relatively small dependence. The incident angle dependence of PSD measured for selectively desorbing ions in the O 1s excitation is shown in figures 13(a)–(c). Obvious incident angle dependence can be also

seen for the site-selective desorption in the O 1s region. It should be noted that since the PIY spectra of the CD_3^+ ion display clear dependence not only in the $\sigma^*(\text{O}-\text{CD}_3)$ but also in the $\sigma^*(\text{C}-\text{OCD}_3)$ excitation, the CD_3^+ ion desorbs selectively even in the $\sigma^*(\text{C}-\text{OCD}_3)$ excitation as a daughter fragment of the OCD_3^+ ion. This site-selective desorption in $\sigma^*(\text{C}-\text{OCD}_3)$ is difficult to distinguish only from the normal PIY spectra in figure 10(b) because of enlargement of the ion yield above the ionization threshold. The same argument is also valid for CD^+ and CD_2^+ ions.

Polarization dependence in the $\sigma^*(\text{O}-\text{CD}_3)$ and $\sigma^*(\text{C}-\text{OCD}_3)$ excitations is summarized in figures 13(d) and (e) for representative ions. In the $\sigma^*(\text{O}-\text{CD}_3)$ excitation, CD_2^+ and CD_3^+ ions show drastic polarization dependence with almost the same trend, while D^+ and OCD^+ are almost independent. On the other hand, the OCD^+ ion is the most dependent one on the polarization in the $\sigma^*(\text{C}-\text{OCD}_3)$ excitation. This variation means that polarization dependence sensitively reflects the desorption process, and ions produced by direct chemical bond breaking desorb with higher dependence.

6. Neutral desorption of core-excited PMMA

Ion desorption for core-excited methyl ester compounds has so far been discussed based on the characteristic site-selectivity. Nevertheless, it should be noted here that the photodesorption yield of neutral products is considered to be much higher than that of ions in core excitation. Besides, neutralization is not negligible in PSD, because electronic interaction between desorbing particles and substrate molecules plays a very important role. Therefore, in order to gain an insight into the true surface photochemistry induced by core excitation, it is necessary to focus the desorbing neutrals as well as to examine the resulting surface species [74].

However, there are limited studies of neutral desorption from core-excited molecules because of much experimental difficulty in detecting neutrals in comparison with ions. Menzel, Feulner and their co-workers have successfully reported the detection of neutral atomic and molecular fragments which desorb from core-excited CO and N_2 molecules adsorbed on transition metal surfaces by using a highly sensitive QMS [10, 32]. Other successful detection of neutral photofragments induced by core-level excitations has also been reported by measuring UV-visible fluorescence even in the gas phase [75, 76], although in this case the detected neutrals are limited to electronically excited ones.

Recent advance of laser technology have developed not only new mass spectroscopy, called femtosecond laser mass spectroscopy (FLMS) [77], but also a newly facilitated experiment combined with SR [78]. In this study, we have introduced a sensitive mass spectroscopy utilizing an ultrashort pulsed laser in combination with TOF-MS to detect neutral products because of the handy introduction to existing facilities and the wide applicability of a laser system [54]. This technique has been applied to the investigation of the neutral photodesorption reaction of the PMMA thin film induced by core excitations.

Figure 14 shows the typical TOF spectrum measured for PMMA at the $\sigma^*(\text{C}-\text{OCH}_3) \leftarrow \text{O } 1\text{s}(\text{OCH}_3)$ excitation. The spectrum was obtained by the subtraction procedure and accordingly indicates

genuine photodesorbing neutral products. Core-excited PMMA produces various photodesorbing neutrals in comparison with ion desorption, mainly H, H₂, CH₃, CH₄, CO, OCH_n, CH₃OH, CH₃CCH₂, CO₂, (CH₃)₂CCH₂, COOCH₃ and HCOOCH₃, which correspond to the previously reported mass spectrum by Tinone *et al* [79]. Note that the broad peaks at 6 and 12 amu (C²⁺ and C⁺) are due to a carbon adhesion tape which was used to fix the sample on a holder. Although the photofragmentation process becomes non-negligible for organic molecules in the experimental condition of the intense laser pulses used (10¹³–10¹⁴ W cm⁻²) [77, 80], the yields of CH and CH₂ are much smaller than CH₃ and the mass pattern of the obtained TOF spectra is similar to the reported mass spectrum by Tinone *et al*.

Figure 15 depicts the yield plots of representative fragments of H, CH₃ and OCH in the C 1s and O 1s excitations together with the TEY and corresponding PIY spectra. The photon energy dependence of all neutral fragments follows the profile of the TEY spectrum but not the PIY spectrum. This result indicates that PSD of neutral products is mainly caused by XESD phenomena and the random energy redistribution in highly excited states, in company with charge transfer by electronic interaction with nearby molecules. It should be mentioned that Menzel and Feulner have reported noteworthy site-selective PSD of neutrals in core-excited N₂ adsorbates by utilizing chemical shift between the N atoms. They have pointed out the importance of the existence of strong surface effects by core excitations through high coupling to substrate to reveal high selectivity besides the dissociative nature of the Auger final states [10]. In the case of PMMA thin film, neutral fragments produced by the indirect process would desorb with much abundance in comparison with those produced by neutralization of the site-selectively desorbing ions. This is supported by the fact that even the MHDA SAM does not show a significant difference with the TEY spectrum in our preliminary measurement. Thus PSD of neutrals does not necessarily reflect the characteristic nature of core excitation except for some specific cases involving a strong interaction with substrate. Ionic dissociation promoted by local Coulomb repulsion between two holes in bonding orbital(s) in the ASD mechanism plays an important role to reveal site-selective dynamics.

7. Summary

This review focuses on the characteristic nature and mechanism of selective chemical bond breaking in core-excited ester compounds: PMMA thin film, a condensed multilayer of MIB as a pseudo-monomer molecule of PMMA, a methyl-ester-terminated SAM (MHDA SAM) and its partially deuterided and an ethyl-ester-terminated SAM (EHDA SAM). For PMMA and the SAMs, exact selective bond breaking was observed as enhanced production of a variety of photodesorbing ions which are well explained by fragmentation followed by COO–R ionic dissociation in the corresponding $\sigma^*(\text{COO-R}) \leftarrow \text{C } 1s$, O 1s(OR) resonant excitations and CO–OR breaking in the $\sigma^*(\text{CO-OR}) \leftarrow \text{O } 1s(\text{OR})$ excitation. On the other hand, condensed MIB does not display enhancement of ion desorption. Moreover, selectivity and relative yield in such resonances improve for the MHDA SAM much more than PMMA and the EHDA SAM. These results indicate the importance of the inter- and intra-molecular environment to make

site-selectivity clear as well as the importance of the resonant core excitation to an antibonding orbital and the subsequent spectator-type Auger decay. Such site-selective excitation takes place within the excited site locally, and even after Auger decay and ionic dissociation/desorption the initial memory of the excited site and its localization character is effectively conserved during PSD process. The fragmentation patterns of desorbing ions show different behaviour in spite of the resonant excitations to the same antibonding orbital. If the primary core-excited atom is included in the removing ion, Auger final energy is concentrated within the ion and used effectively for further fragmentation. In contrast, if the core-excited atom is not included in the removing ion, Auger final energy easily diffuses into a remaining part on the surface and is not effectively used for the fragmentation. From the viewpoint of controlling chemical reactions, we can differentiate these two different types of fragmentation, the bond scission with further fragmentation named 'hard-cut' and that with less fragmentation named 'soft-cut', respectively. The above findings are also supported by polarization-dependent measurements of ionic PSD.

Direct ion desorption initiated by soft x-ray irradiation is usually disturbed by accompanying indirect desorption due to statistical energy relaxation and XESD. Such direct and indirect processes are analytically evaluated for site-specific C 1s resonances. High quality of the direct process of 90–95% is derived for COO–CH₃ bond breaking of the MHDA SAM, which is considered to be mainly disturbed by statistical energy delocalization because the XESD process is reduced in the SAM.

Various neutral products desorbing from core-excited PMMA show almost the same photon energy dependence as the TEY spectrum but not each PIY. The result indicates that PSD of neutral products is mainly caused by an indirect process rather than neutralization of desorbing ions. Ionic dissociation locally promoted by Coulomb repulsion in the ASD mechanism plays an important role to reveal site-selective dynamics.

As mentioned above, we can conclude that the ionic dissociation process on the surface is important to clarify the characteristic nature and mechanism of core-electron excitation. Although there are still problems which should be overcome, like improvement of direct processes and restraint of indirect ionic and neutral desorption, the concept of the 'molecular scalpel' illustrated in figure 1 is realizable in principle by using a tunable soft x-ray so that we expect to apply this technique to the future modification on the atomic level in surface processes.

Acknowledgements

The authors wish to thank the staff of the Photon Factory and HiSOR for stable operation of the SR ring. This work was performed under the approval of the Photon Factory Programme Advisory Committee (proposal Nos 2002G273 and 2004G314). The present research was supported by a Grant-in-Aid on Research for the Future 'Photoscience' from the Japan Society for the Promotion of Science (JSPS-RFTF-98P-01202) and Grants-in-Aid from the Ministry of Education, Culture, Sports, Science and Technology of Japan (15750011 and 16205002).

References

- [1] Stöhr J 1992 *NEXAFS Spectroscopy* (Berlin: Springer)
- [2] Bachrach R Z (ed) 1992 *Synchrotron Radiation Research -Advances in surface and interface science-* (New York: Plenum)
- [3] Ramaker D E, White C T and Murday J S 1981 *J. Vac. Sci. Technol.* **18** 748
Ramaker D E, White C T and Murday J S 1982 *Phys. Lett. A* **84** 211
- [4] Eberhardt W, Sham T K, Carr R, Krummacher S, Strongin M, Weng S L and Wesner D, 1983 *Phys. Rev. Lett.* **50** 1038
- [5] Ueno N and Tanaka K 1997 *Jpn. J. Appl. Phys.* **36** 7605
- [6] Tanaka K, Sako E O, Ikenaga E, Isari K, Sardar S A, Wada S, Sekitani T, Mase K and Ueno N 2001 *J. Electron Spectrosc. Relat. Phenom.* **119** 255
- [7] Nagaoka S, Mase K, Nakamura A, Nagao M, Yoshinobu J and Tanaka S 2002 *J. Chem. Phys.* **117** 3961, and references therein
Nagaoka S and Mase K 2005 *Surf. Sci.* **593** 276
- [8] Baba Y 2003 *Low Temp. Phys.* **29** 228, and references therein
- [9] Mase K, Nagasono M, Tanaka S, Sekitani T and Nagaoka S 2003 *Low Temp. Phys.* **29** 243, and references therein
- [10] Menzel D and Feulner P 2001 *J. Phys.: Condens. Matter* **13** 11249, and references therein
- [11] Nagaoka S, Koyano I, Ueda K, Shigemasa E, Sato Y, Yagishita A, Nagata T and Hayaishi T 1989 *Chem. Phys. Lett.* **154** 363
Nagaoka S, Tamenori Y, Hino M, Kakiuchi T, Ohshita J, Okada K, Ibuki T and Suzuki I H 2005 *Chem. Phys. Lett.* **412** 459
Nagaoka S, Tamura A, Fujii A, Ohshita J, Okada K, Ibuki T, Suzuki I H, Ohashi H, Tamenori Y 2005 *Int. J. Mass Spectrom.* **247** 101
- [12] Morin P, Lebrun T and Lablanquie P 1989 *Bull. Soc. Roy. Sci. Liege* **58** 135
Morin P, Simon M, Miron C, Leclercq N, Kukk E, Bozek J. D and Berrah N 2000 *Phys. Rev. A* **61** 050701
- [13] Nenner I, Morin P, Lablanquie P, Simon M, Lévassieur N and Millie P 1990 *J. Electron Spectrosc. Relat. Phenom.* **52** 623
Schmelz H C, Reynaud C, Simon M and Nenner I 1994 *J. Chem. Phys.* **101** 3742
Miron C, Simon M, Leclercq N, Hansen D L and Morin P 1998 *Phys. Rev. Lett.* **81** 4104
Le Guen K, Ahmad M, Céolin D, Lablanquie P, Miron C, Penent F, Morin P and Simon M 2005 *J. Chem. Phys.* **123** 084302
- [14] Thissen R, Simon M and Franskin M -J 1994 *J. Chem. Phys.* **101** 7548
- [15] Suzuki I H, Bozek J D and Saito N 1994 *Chem. Phys.* **182** 81
Saito N, Bozek J D and Suzuki I H 1994 *Chem. Phys.* **188** 367
Suzuki I H, Saito N and Bozek J D 1994 *Int. J. Mass Spectrom. Ion Proc.* **136** 55
Suzuki I H and Saito N 1998 *Chem. Phys.* **234** 255
Suzuki I H, Saito N and Bozek J D 1999 *J. Electron Spectrosc. Relat. Phenom.* **101-103** 69
- [16] Boo B H, Park S M and Koyano I 1995 *J. Phys. Chem.* **99** 13362
Boo B H, Liu Z, Lee S Y and Koyano I 1998 *J. Phys. Chem. A* **102** 8261
Boo B H, Liu Z and Koyano I 2000 *J. Phys. Chem. A* **104** 1474
Boo B H, Lee J K and Saito N 2002 *J. Phys. Chem. A* **106** 1511
Boo B H, Saito N, Suzuki I H and Koyano I 2002 *J. Electron Spectrosc. Relat. Phenom.* **123** 73
Boo B H, Saito N, Suzuki I H and Koyano I 2002 *J. Mol. Struct.* **610** 17
Boo B H and Saito N 2002 *J. Electron Spectrosc. Relat. Phenom.* **127** 139
Boo B H and Saito N 2003 *J. Electron Spectrosc. Relat. Phenom.* **128** 119
- [17] Erman P, Karawajczyk A, Köble U, Rachlew-Käellne E and Franzén K Y 1996 *Phys. Rev. A* **53** 1407
Erman P, Karawajczyk A, Rachlew E, Stankiewicz M and Franzén K Y 1997 *J. Chem. Phys.* **107** 10827
Franzén K Y, Erman P, Karawajczyk A, Rachlew E, Hatherly P A and Stankiewicz M 1999 *J. Chem. Phys.* **110** 3621
Stankiewicz M, Winiarczyk P, Riu J R I, Alvarez J, Erman P, Karawajczyk A, Rachlew E, Kukk E, Huttula M and Hatherly P 2002 *Surf. Rev. Lett.* **9** 117

- Rius i Riu J, Garcia E M, Ruiz J A, Erman P, Hatherly P, Rachlew E and Stankiewicz M 2003 *Phys. Rev. A* **68** 022715
- [18] Fainelli E, Maracci F, Platania R and Avaldi L 1998 *J. Electron Spectrosc. Relat. Phenom.* **87** 169
- [19] Hitchcock A P, Neville J J, Jürgensen A and Cavell R G 1998 *J. Electron Spectrosc. Relat. Phenom.* **88-91** 71
- [20] Ibuki T, Okada K, Gejo T, Saito K 1999 *J. Electron Spectrosc. Relat. Phenom.* **101-103** 149
 Gejo T, Okada K, Ibuki T and Saito N 1999 *J. Phys. Chem. A* **103** 4598
 Ibuki T, Okada K, Saito K and Gejo T 2000 *J. Electron Spectrosc. Relat. Phenom.* **107** 39
 Ibuki T, Okada K, Tanimoto S, Saito K and Gejo T 2002 *J. Electron Spectrosc. Relat. Phenom.* **123** 323
 Okada K, Tanimoto S, Morita T, Saito K, Ibuki T and Gejo T 2003 *J. Phys. Chem. A* **107** 8444
 Ibuki T, Okada K, Takahashi M, Samori S, Goya T, Senba Y, Yoshida H, Hiraya A and Ohno K 2005 *J. Electron Spectrosc. Relat. Phenom.* **143** 21
 Ibuki T, Shimada Y, Hashimoto R, Nagaoka S, Hino M, Okada K, Suzuki I H, Morishita Y and Tamenori Y 2005 *Chem. Phys.* **314** 119
- [21] Naves de Brito A, Feifel R, Mocellin A, Machado A B, Sundin S, Hjelte I, Sorensen S L and Björneholm O 1999 *Chem. Phys. Lett.* **309** 377
 Naves de Brito A, Sundin S, Marinho R R, Hjelte I, Fraguas G, Gejo T, Kosugi N, Sorensen S and Björneholm O 2000 *Chem. Phys. Lett.* **328** 177
- [22] Ueda K, Simon M, Miron C, Leclercq N, Guillemin R, Morin P and Tanaka S 1999 *Phys. Rev. Lett.* **83** 3800
- [23] Stolte W C, Ohrwall G, Sant'Anna M M, Dominguez L I, Dang L T N, Piancastelli M N and Lindle D W 2002 *J. Phys. B* **35** L253
 Yu S -W, Stolte W C, Örwall G, Guillemin R, Piancastelli M N and Lindle D W 2003 *J. Phys. B* **36** 1255
 Piancastelli M N, Stolte W C, Guillemin R, Wolska A, Yu S -W, Sant'Anna M M and Lindle D W 2005 *J. Chem. Phys.* **122** 94312
- [24] Lago A F, Santos A C F and De Souza G G B 2004 *J. Chem. Phys.* **120** 9547
- [25] Chen J M, Lu K T, Lee J M, Ma C I and Lee Y Y 2004 *Phys. Rev. Lett.* **92** 243002
 Chen J M, Lu K T, Lee J M, Ho S C, Chang H W and Lee Y Y 2005 *J. Electron Spectrosc. Relat. Phenom.* **144-147** 171
 Chen J M, Lu K T, Lee J M, Ho S C and Chang H W 2005 *Phys. Rev. A* **72** 32706
- [26] Erben M F, Romano R M, Della V and Della Védova C O 2005 *J. Phys. Chem. A* **109** 304
 Erben M F, Geronés M, Romano R M and Della Védova C O 2006 *J. Phys. Chem. A* **110** 875
- [27] Azuma Y, Mishima Y, Senba Y, Yoshida Y and Hiraya A 2005 *J. Electron Spectrosc. Relat. Phenom.* **144** 183
- [28] Liu X J *et al* 2005 *Phys. Rev. A* **72** 042704
- [29] Ultra-fast dissociation in core-excited states of gaseous molecules can be also classified into site-specific fragmentation. For example, see Björneholm O 2001 *J. Chem. Phys.* **115** 4139, and references therein
- [30] Treichler R, Riedl W, Wurth W, Feulner P and Menzel D 1985 *Phys. Rev. Lett.* **54** 462
- [31] Menzel D, Feulner P, Treichler R, Umbach E and Wurth W 1987 *Phys. Scr.* **T17** 166
 Treichler R, Riedl W, Feulner P and Menzel D 1991 *Surf. Sci.* **243** 239
- [32] Frigo S P, Feulner P, Kassühlke B, Keller C and Menzel D 1998 *Phys. Rev. Lett.* **80** 2813
 Feulner P, Ecker M, Romberg R, Weimar R and Föhlisch 2002 *Surf. Rev. Lett.* **9** 759
- [33] Coulman D, Puschmann A, Höfer U, Steinrück H -P, Wurth W, Feulner P and Menzel D 1990 *J. Chem. Phys.* **93** 58
- [34] Eberhardt W, Colbow K M, Gao Y, Rogers D and Tiedje T 1992 *Phys. Rev. B* **46** 12388
- [35] Sekiguchi T, Ikeura H, Tanaka K, Obi K, Ueno N and Honma K 1995 *J. Chem. Phys.* **102** 1422
 Sekiguchi T, Ikeura H, Tanaka K and Obi K 1996 *J. Electron Spectrosc. Relat. Phenom.* **80** 65
 Sekiguchi T, Sekiguchi H I and Tanaka K 1997 *Surf. Sci.* **390** 199
 Wu G, Baba Y, Sekiguchi T and Shimoyama I 2001 *J. Synchrotron. Rad.* **8** 469
 Baba Y, Wu G, Sekiguchi T and Shimoyama I 2001 *J. Vac. Sci. Technol. A* **19** 1485
 Baba Y, Sekiguchi T and Shimoyama I 2002 *Surf. Rev. Lett.* **9** 77
 Sekiguchi H I, Sekiguchi T, Kitajima, Y and Baba Y 2001 *Appl. Surf. Sci.* **169-170** 282
 Sekiguchi H I, Sekiguchi T and Koike M 2005 *J. Electron Spectrosc. Relat. Phenom.* **144-147** 453

- Sekiguchi H I, Sekiguchi T, Baba Y, Imamura M, Matsubayashi N and Shimada H 2005 *Surf. Sci.* **593** 303
- [36] Sekiguchi T, Sekiguchi H I, Imamura M, Matsubayashi N, Shimada H and Baba Y 2001 *Surf. Sci.* **482-485** 279
 Sekiguchi T, Sekiguchi H I, Imamura M, Matsubayashi N and Shimada H 2001 *Appl. Surf. Sci.* **169-170** 287
 Sekiguchi T, Sekiguchi H I and Baba Y 2003 *Surf. Sci.* **532-535** 1079
 Sekiguchi T, Baba Y, Shimoyama I and Nath K G 2005 *J. Electron Spectrosc. Relat. Phenom.* **144-147** 437
 Sekiguchi T, Baba Y, Shimoyama I, Wu G and Kitajima Y 2005 *Surf. Sci.* **593** 310
- [37] Chen J M, Klauser R, Yang S and Wen C -R 1995 *Chem. Phys. Lett.* **246** 285
 Yang S C, Chen J M, Wen C -R, Hsu Y J, Lee Y P, Chuang T J and Liu Y C 1997 *Surf. Sci.* **385** L1010
 Chen J M and Lu K T 2001 *Phys. Rev. Lett.* **86** 3176
 Chen J M, Lu K T and Lee J M 2003 *J. Chem. Phys.* **118** 5087
- [38] Friedrich C M, Wilkes J, Palmer R E, Bennett S L, MacDonald M A and Lamont C L A, Foord J S 1995 *Chem. Phys. Lett.* **247** 348
- [39] Carbone M, Piancastelli M N, Zanoni R, Comtet G, Dujardin G and Hellner L 1997 *Surf. Sci.* **390** 219
 Carbone M, Piancastelli M N, Casaletto M P, Zanoni R, Comtet G, Dujardin G and Hellner L 2003 *Chem. Phys.* **289** 93
- [40] Taylor D P, Simpson W C, Knutsen K, Henderson M A and Orlando T M 1998 *Appl. Surf. Sci.* **127-129** 101
- [41] Simpson W C, Wang W K, Yarmoff J A and Orlando T M 1999 *Surf. Sci.* **423** 225
- [42] Parent P, Laffon C and Bournel F 2000 *J. Chem. Phys.* **112** 986
- [43] Okudaira K K, Ohara K, Setoyama H, Suzuki T, Sakamoto Y, Imamura M, Hasegawa S, Mase K and Ueno N 2003 *Nucl. Instr. and Meth. in Phys. Res. B* **199** 265
 Okudaira K K, Setoyama H, Yagi H, Mase K, Kera S, Kahn A and Ueno N 2004 *J. Electron Spectrosc. Relat. Phenom.* **137-140** 137
 Okudaira K K, Watanabe T, Kera S, Kobayashi E, Mase K and Ueno N 2005 *J. Electron Spectrosc. Relat. Phenom.* **144-147** 461
 Okudaira K K, Kobayashi E, Kera S, Mase K and Ueno N 2005 *Surf. Sci.* **593** 297
- [44] Kobayashi E, Isari K and Mase K 2003 *Surf. Sci.* **528** 255
 Nambu A, Kobayashi E, Mori M, Okudaira K K, Ueno N and Mase K 2005 *Surf. Sci.* **593** 269
 Kobayashi E, Nambu A and Mase K, 2005 *Surf. Sci.* **593** 291
- [45] Tanaka S, Mase K and Nagaoka S 2004 *Surf. Sci.* **572** 43
- [46] Hellner L, Comtet G, Ramage M J, Bobrov K, Carbone M and Dujardin G 2003 *J. Chem. Phys.* **119** 515
- [47] Rocco M L M, Faraudo G S, Pontes F C, Pinho R R, Ferreira M and de Souza G G B 2004 *Chem. Phys. Lett.* **393** 213
 Rocco M L M, Faraudo G S, Pinho R R, Ferreira M, Pontes F C and de Souza G G B 2004 *J. Electron Spectrosc. Relat. Phenom.* **141** 1
- [48] Tinone M C K, Tanaka K, Maruyama J, Ueno N, Imamura M and Matsubayashi N 1994 *J. Chem. Phys.* **100** 5988
- [49] Sekitani T, Ikenaga E, Fujii K, Mase K, Ueno N and Tanaka K 1999 *J. Electron Spectrosc. Relat. Phenom.* **101-103** 135
- [50] Ikenaga E, Isari K, Kudara K, Yasui Y, Sardar S A, Wada S, Sekitani T, Tanaka K, Mase K and Tanaka S 2001 *J. Chem. Phys.* **114** 2751
 Ikenaga E, Kudara K, Kusaba K, Isari K, Sardar S A, Wada S, Mase K, Sekitani T and Tanaka K 2001 *J. Electron Spectrosc. Relat. Phenom.* **114-116** 585
- [51] Sako E O, Kanameda Y, Ikenaga E, Mitani M, Takahashi O, Saito K, Iwata S, Wada S, Sekitani T and Tanaka K 2001 *J. Electron Spectrosc. Relat. Phenom.* **114-116** 591
- [52] Tanaka K, Tinone M C K, Ikeura H, Sekiguchi T and Sekitani T 1995 *Rev. Sci. Instrum.* **66** 1474
- [53] Wada S, Sumii R, Kizaki H, Iizuka Y, Matsumoto Y, Sekitani T and Tanaka K 2005 *Surf. Sci.* **593** 283
- [54] Wada S, Matsumoto Y, Kohno M, Sekitani T and Tanaka K 2004 *J. Electron Spectrosc. Relat. Phenom.* **137-140** 211

- [55] Wada S, Sako E O, Sumii R, Waki S, Isari K, Sekiguchi T, Sekitani T and Tanaka K 2003 *Nucl. Instr. and Meth. B* **199** 361
Wada S, Sumii R, Isari K, Waki S, Sako E O, Sekiguchi T, Sekitani T and Tanaka K 2003 *Surf. Sci.* **528** 242
- [56] Wada S, Sumii R, Kizaki H, Matsumoto Y and Tanaka K to be published
- [57] Sumii R, Wada S, Kizaki H, Matsumoto Y and Tanaka K to be published
- [58] Sekitani T, Kusaba K, Morita K, Nanbu Y, Isari K, Ikenaga E, Wada S and Tanaka K 2003 *Surf. Sci.* **532-535** 267
- [59] Tanaka K, Kizaki H, Sumii R, Matsumoto Y and Wada S 2006 *Radiat. Phys. Chem.* in press
- [60] Kizaki H, Wada S, Sako E O, Sumii R, Waki S, Isari K, Sekitani T, Sekiguchi T and Tanaka K 2005 *J. Electron Spectrosc. Relat. Phenom.* **144-147** 447
- [61] Nelson M C, Murakami J, Anderson S L and Hanson D M 1987 *J. Chem. Phys.* **86** 4442
- [62] Suzuki I H and Saito N 2000 *Chem. Phys.* **253** 351
Suzuki I H and Saito N 2000 *Int. J. Mass Spectrom.* **198** 165
- [63] Dubois L H and Nuzzo R G 1992 *Annu. Rev. Phys. Chem.* **43** 437
- [64] Ulman A 1996 *Chem. Rev.* **96** 1533
- [65] Amemiya K, Kondoh H, Yokoyama T and Ohta T 2002 *J. Electron Spectrosc. Relat. Phenom.* **124** 151
- [66] Batson P E 1993 *Phys. Rev. B* **48** 2608
- [67] Prince K C, Avaldi L, Coreno M, Camilloni R and Simone M 1999 *J. Phys. B* **32** 2551
- [68] Urquhart S G and Ade H 2002 *J. Phys. Chem. B* **106** 8531
Dhez O, Ade H and Urquhart S G 2003 *J. Electron Spectrosc. Relat. Phenom.* **128** 85
- [69] Nuzzo R G, Dubois L H and Allara D L 1990 *J. Am. Chem. Soc.* **112** 558
- [70] Bagus P S, Weiss K, Schertel A, Wöll Ch, Braun W, Hellwig C and Jung C 1996 *Chem. Phys. Lett.* **248** 129
- [71] Heinrich N, Drewello T, Burgers P C, Morrow J C, Schmidt J, Kulik W, Terlouw J K and Schwarz H 1992 *J. Am. Chem. Soc.* **114** 3776
- [72] Rosenstock H M, Draxl K, Steiner B W and Herron J T 1977 Energetics of gaseous ions *J. Phys. Chem. Ref. Data* **6** Suppl. 1
- [73] Jaeger R, Stöhr J and Kendelewicz J 1983 *Phys. Rev. B* **28** 1145
Jaeger R, Stöhr J and Kendelewicz J 1983 *Surf. Sci.* **134** 547
- [74] Rosenberg R A and Frigo S P 2002 *Chemical Applications of Synchrotron Radiation Part I: Dynamics and VUV Spectroscopy* ed Sham T K (New Jersey: World Scientific) Chapter 9
- [75] Rosenberg R A, Wen C -R, Tan K and Chen J -M 1990 *J. Chem. Phys.* **92** 5196
- [76] Marquette A, Gisselbrecht M, Benten W and Meyer M 2000 *Phys. Rev. A* **62** 022513
- [77] Smith D J, Ledingham K W D, Singhal R P, Kilic H S, McCanny T, Langley A J, Taday P F and Kosmidis C 1998 *Rapid Commun. Mass Spectrom.* **12** 813
- [78] For example, see Tadjeddine A *et al* 1998 *J. Synchrotron Rad.* **5** 293
Niikura H, Mizutani M and Mitsuke K 2000 *Chem. Phys. Lett.* **317** 45
- [79] Tinone M C K, Tanaka K and Ueno N 1995 *J. Vac. Sci. Technol. A* **13** 1885
- [80] Harada H, Shimizu S, Yatsuhashi T, Sakabe S, Izawa Y and Nakashima N 2001 *Chem. Phys. Lett.* **342** 563

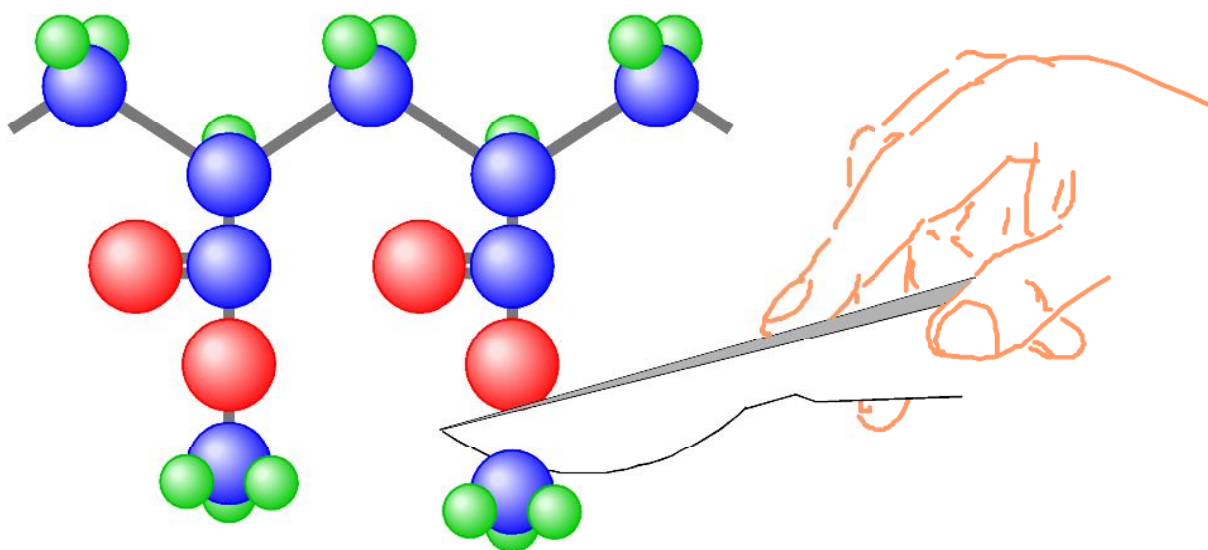


Figure 1. Conceptual illustration of a 'molecular scalpel', where a tunable soft x-ray is used as an atomic level scalpel.

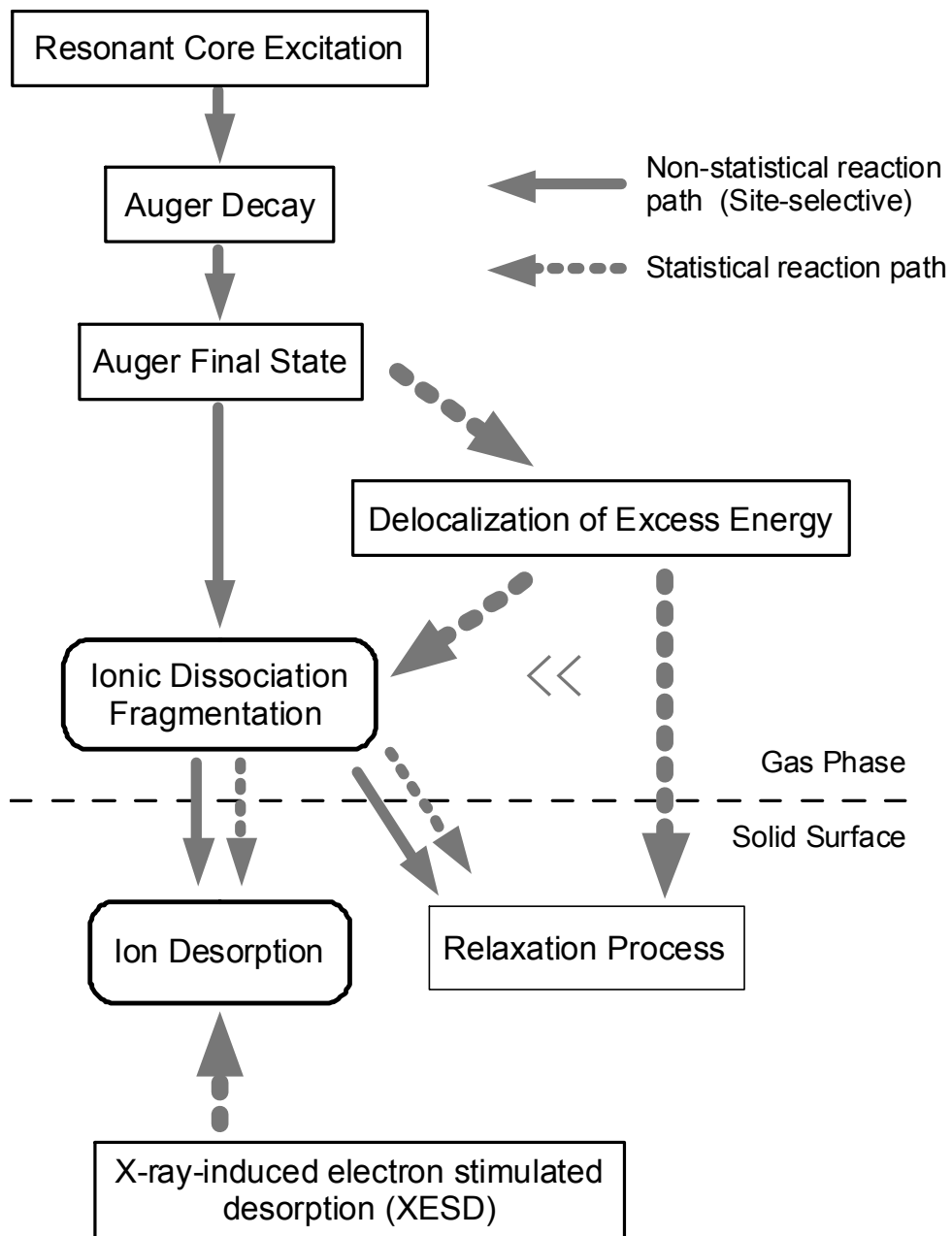


Figure 2. Scheme of hypothetical reaction paths initiated by core excitation in gas phase and on solid surface.

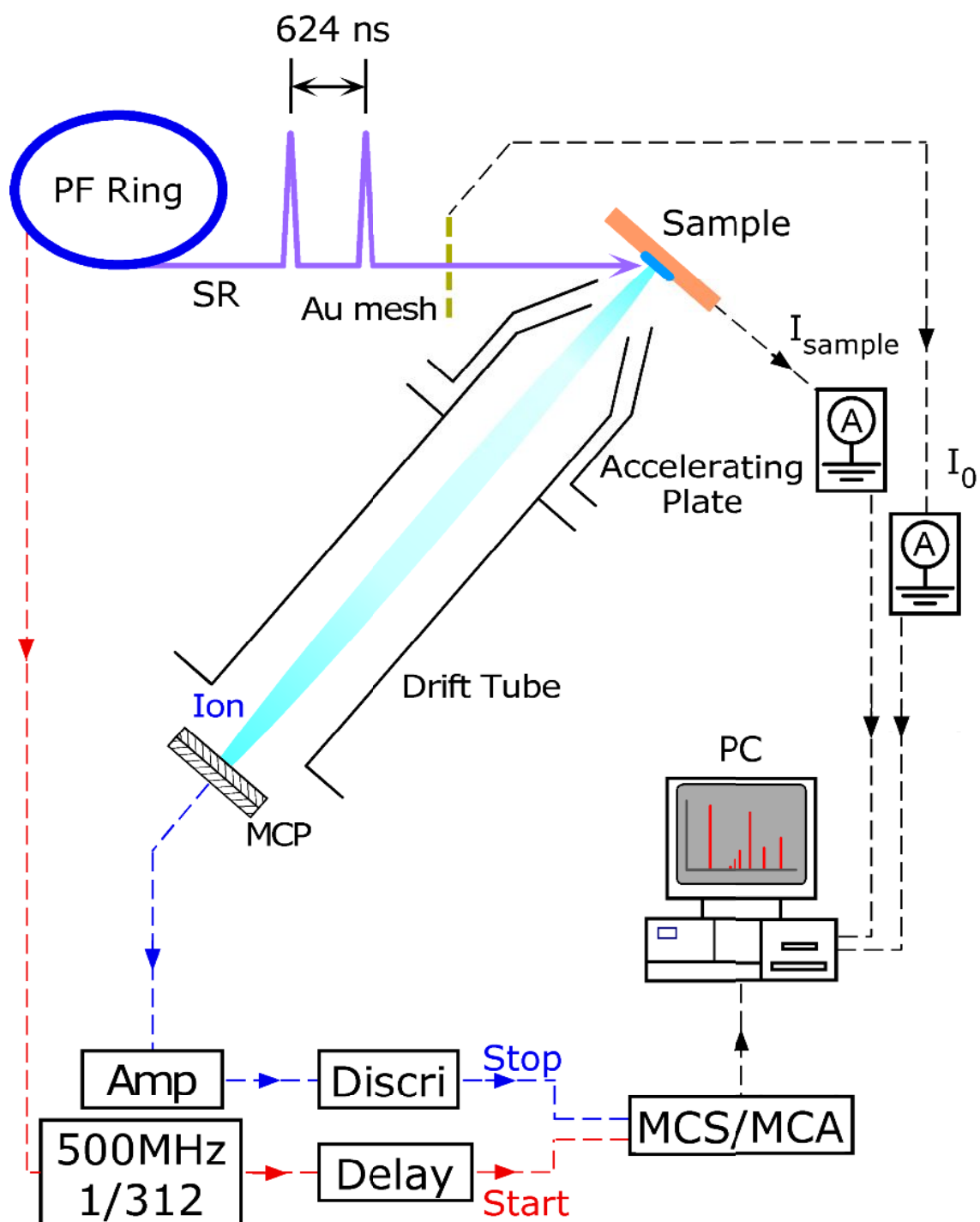


Figure 3. Schematic drawing of experimental set-up for detection of total electrons and desorbing ions, which mainly consists of pulsed SR light (624 ns interval), TOF-MS and data acquisition system. A: ammeter, Amp: fast-preamplifier, Discr: discriminator, MCS/MCA: multichannel scaler and multichannel analyser.

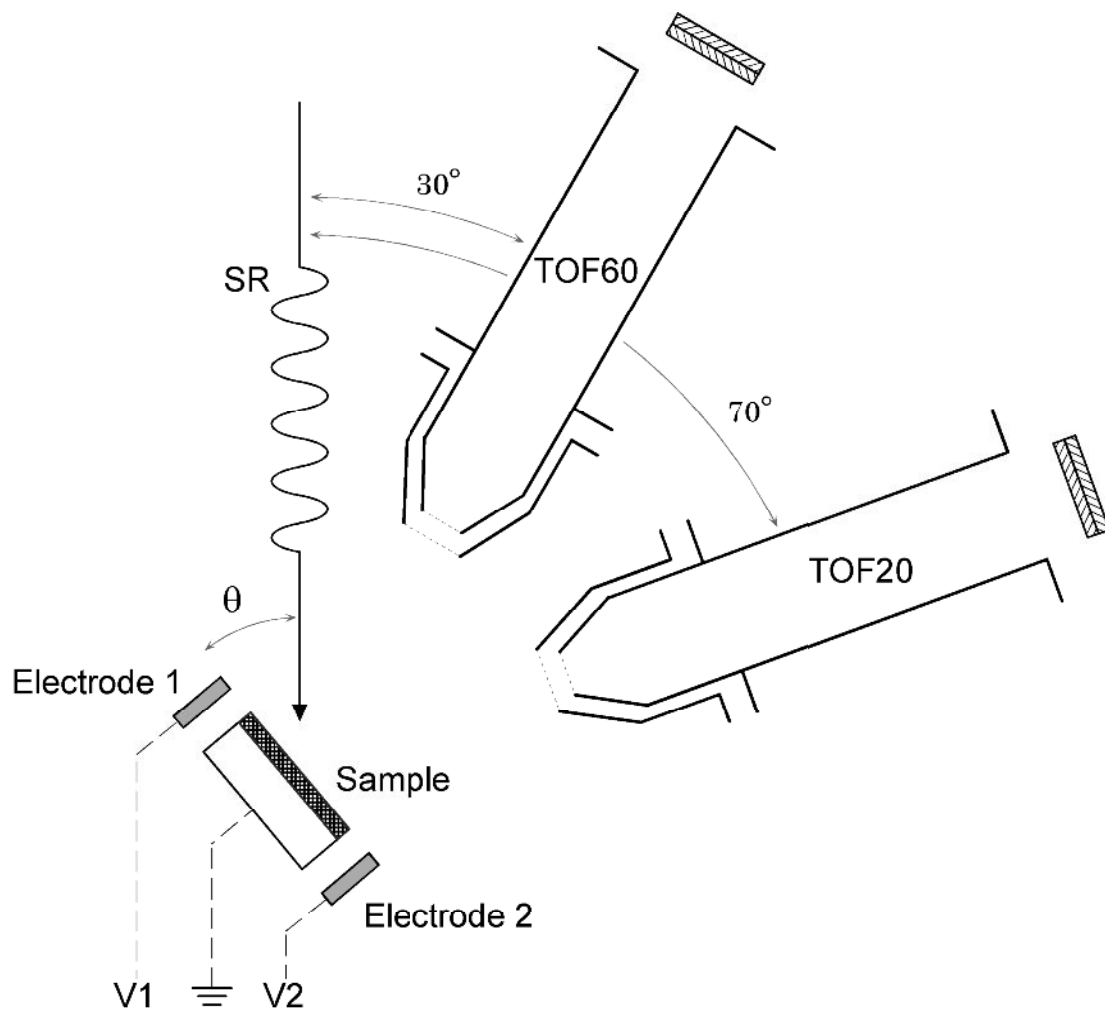


Figure 4. Schematic drawing of experimental set-up for polarization-dependent PSD measurement, which consists of two equivalent TOF-MS devices combined with two correction electrodes on both sides of the sample holder.

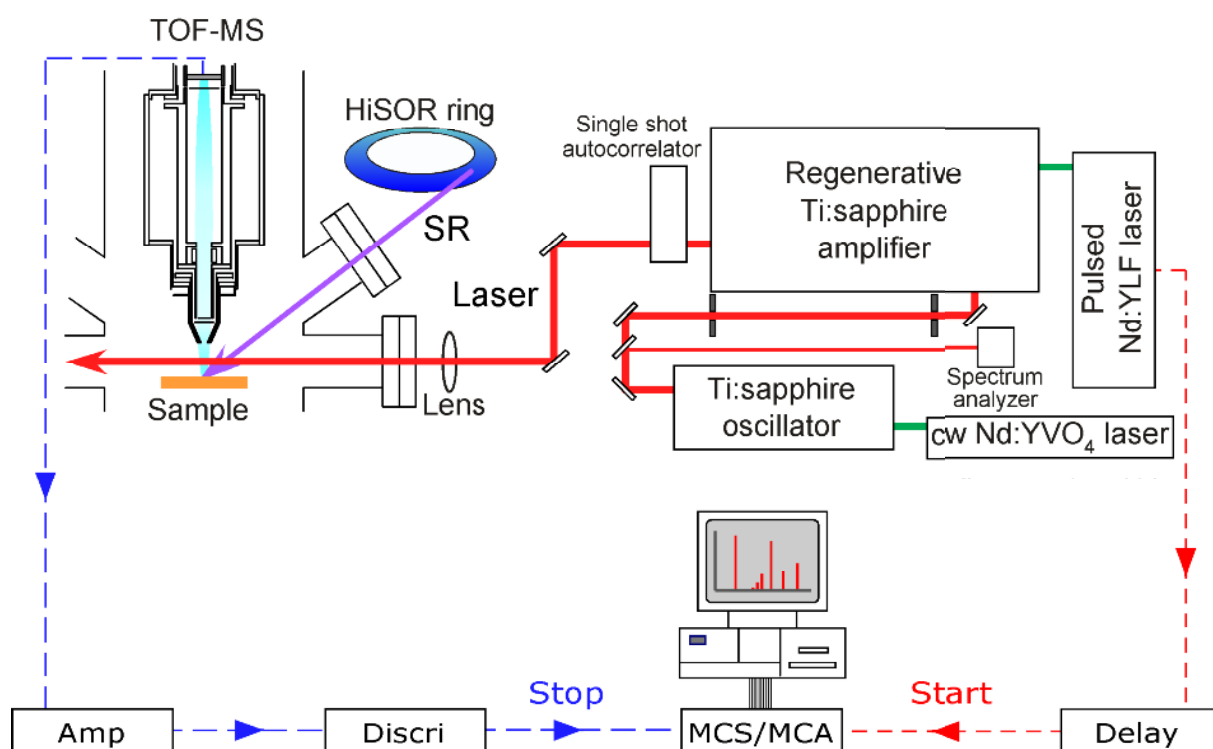


Figure 5. Schematic drawing of experimental set-up for neutral detection system, which mainly consists of SR, a femtosecond laser system, TOF-MS and a data acquisition system. The incident angle of SR light is 35° from a sample surface and the laser is introduced in parallel with the surface.

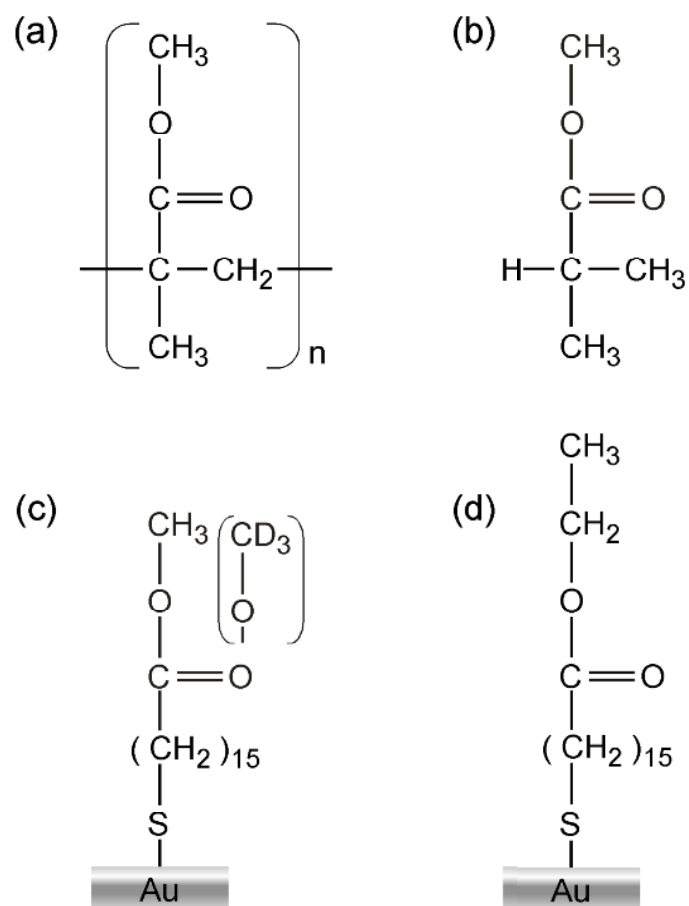


Figure 6. Molecular structures of ester compounds used in this experiment. (a) PMMA, (b) methyl isobutyrate, (c) methyl ester terminated SAM and its partial deuteride and (d) ethyl ester terminated SAM.

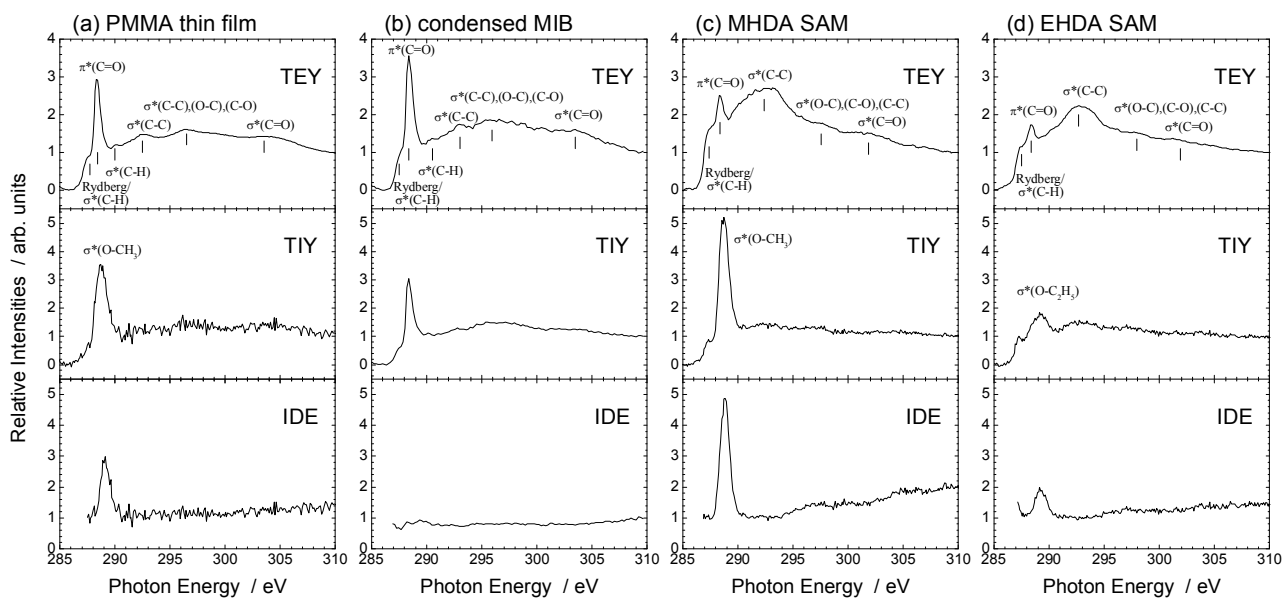


Figure 7. Total electron yield (TEY), total ion yield (TIY) and ion desorption efficiency (IDE) spectra of (a) PMMA thin film, (b) condensed MIB, (c) MHDA SAM and (d) EHDA SAM in the C 1s region. Assignments for typical transitions are shown in each spectrum.

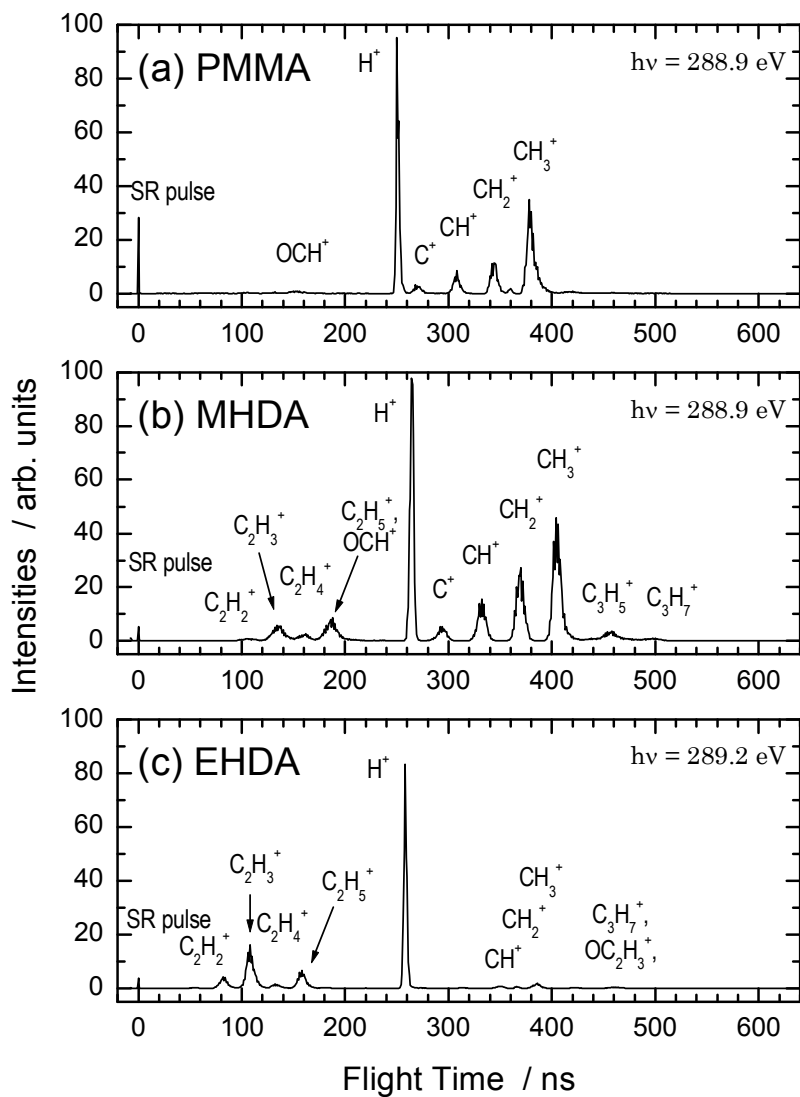


Figure 8. Typical TOF spectra of ionic photofragments desorbing from core-excited (a) PMMA and (b) MHDA SAM at the $\sigma^*(\text{O}-\text{CH}_3)$ excitations and (c) EHDA SAM at the $\sigma^*(\text{O}-\text{C}_2\text{H}_5)$ excitation. As the experiment was performed under single bunch operation of the Photon Factory storage ring (624 ns interval), each spectrum is a superposition of the TOF spectra triggered by several cycles of SR light. Mass assignments are shown in each spectrum.

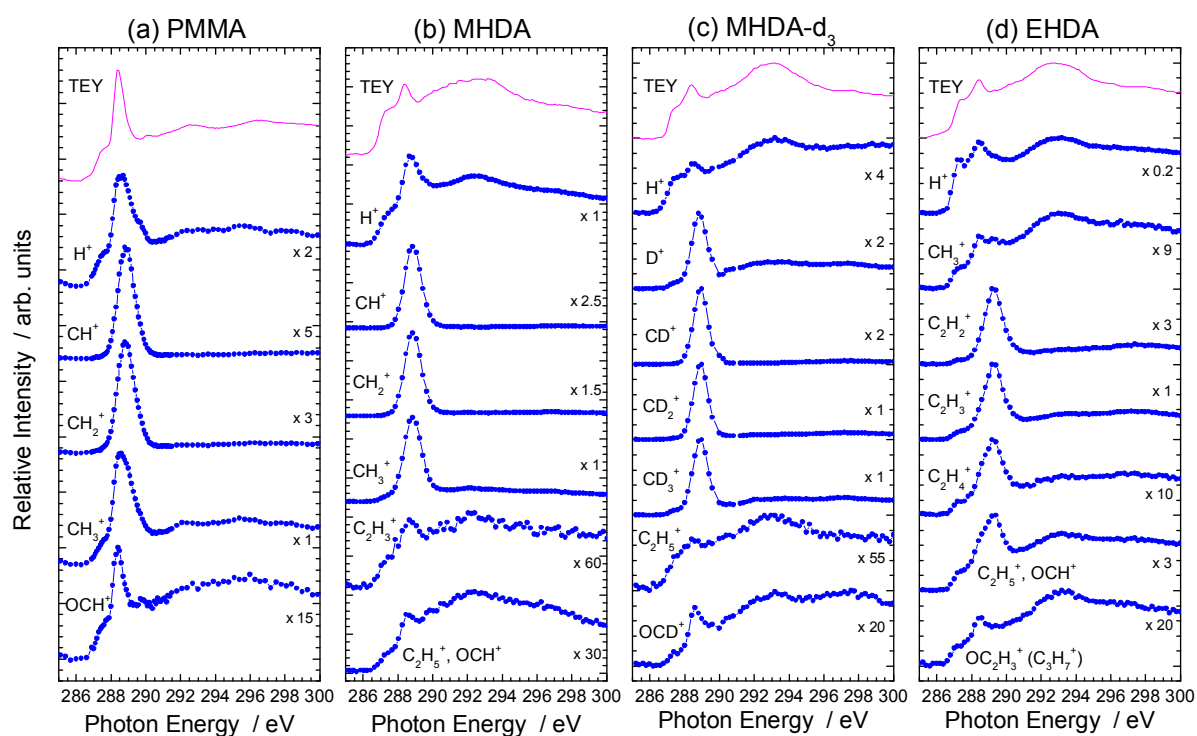


Figure 9. Representative PIY spectra of (a) PMMA, (b) an MHDA SAM, (c) an MHDA- d_3 SAM and (d) an EHDA SAM in the C 1s region. TEY spectra are also shown at the top. Spectra were measured at the SR incident angle of 20° from the surface. The intensities of the spectra are multiplied approximately by the numeral values given on the right side.

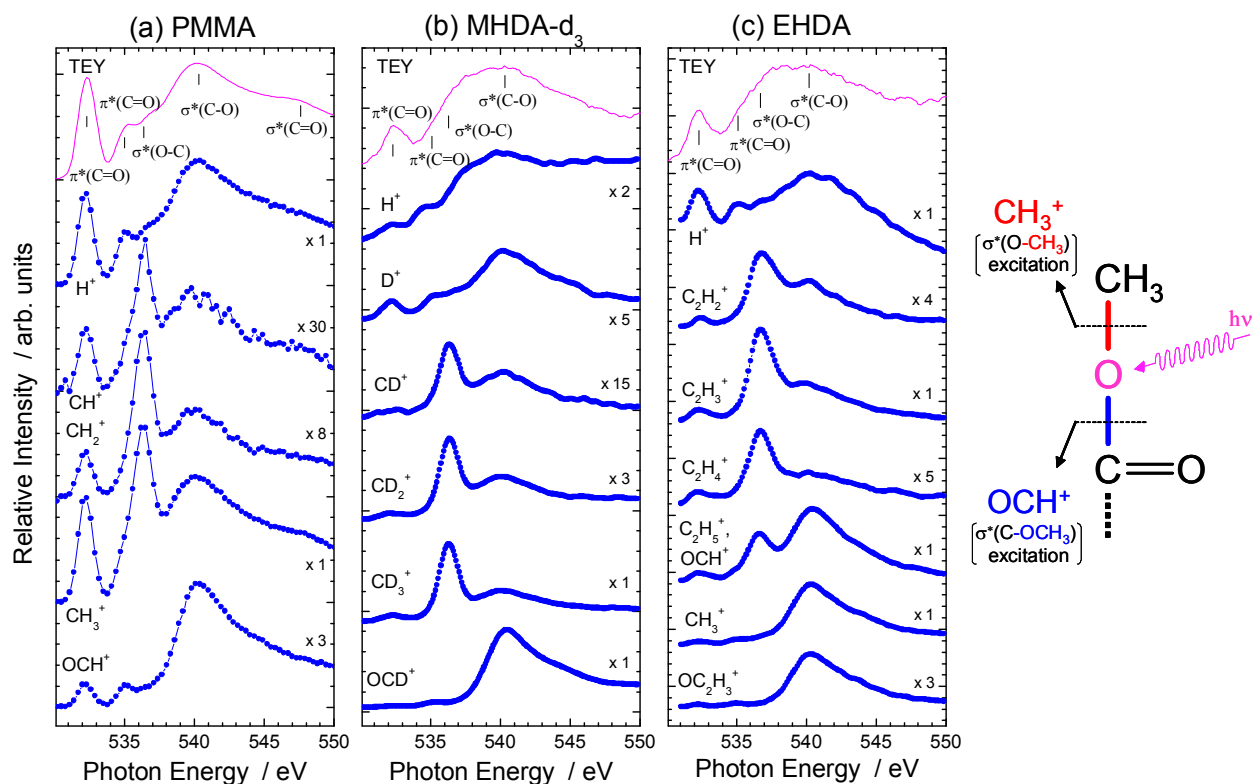


Figure 10. Representative PIY spectra of (a) PMMA, (b) the MHDA- d_3 SAM and (c) the EHDA SAM in the O 1s region. TEY spectra are also shown at the top. Spectra were measured at the SR incident angle of 20° from the surface. Intensities of spectra are multiplied approximately by numeral values given on the right side. (Right) Schematic drawing of site-selective bond breaking in the methyl ester group induced by resonant core excitations.

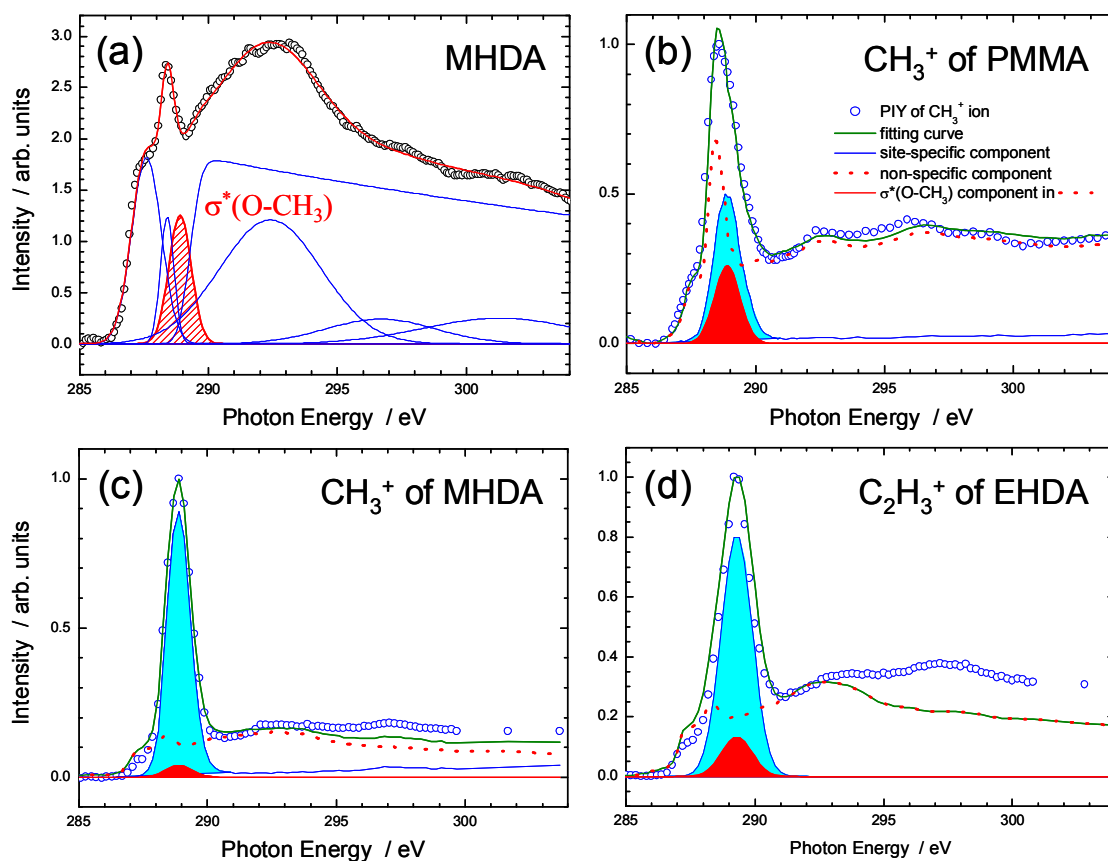


Figure 11. (a) Peak-fitting analysis for the TEY spectrum of the MHDA SAM in the C 1s region. The slash-marked peak corresponds to the component of $\sigma^*(\text{O-CH}_3)$ excitation. (b)–(d) Typical examples of quantitative evaluation for PIY spectra (\circ) of (b) CH_3^+ of PMMA, (c) CH_3^+ of the MHDA SAM and (d) C_2H_3^+ of the EHDA SAM. Light grey (sky-blue) shaded peaks are intensity-modified PIY spectra of each CH^+ (Gauss curve for (d)), which correspond to the components from direct dissociation processes at $\sigma^*(\text{O-CH}_3, \text{O-C}_2\text{H}_5)$ excitations. Dotted (red) lines are modified TEY spectra for each sample and dark grey (red) shaded peaks are $\sigma^*(\text{O-CH}_3, \text{O-C}_2\text{H}_5)$ components of TEY spectra, which correspond to the components from indirect dissociation. Thick lines (green) are reproduced PIY spectra by superposition of the moderately weighted PIY and TEY spectra. (c) and (d) are the case where the direct components are underestimated.

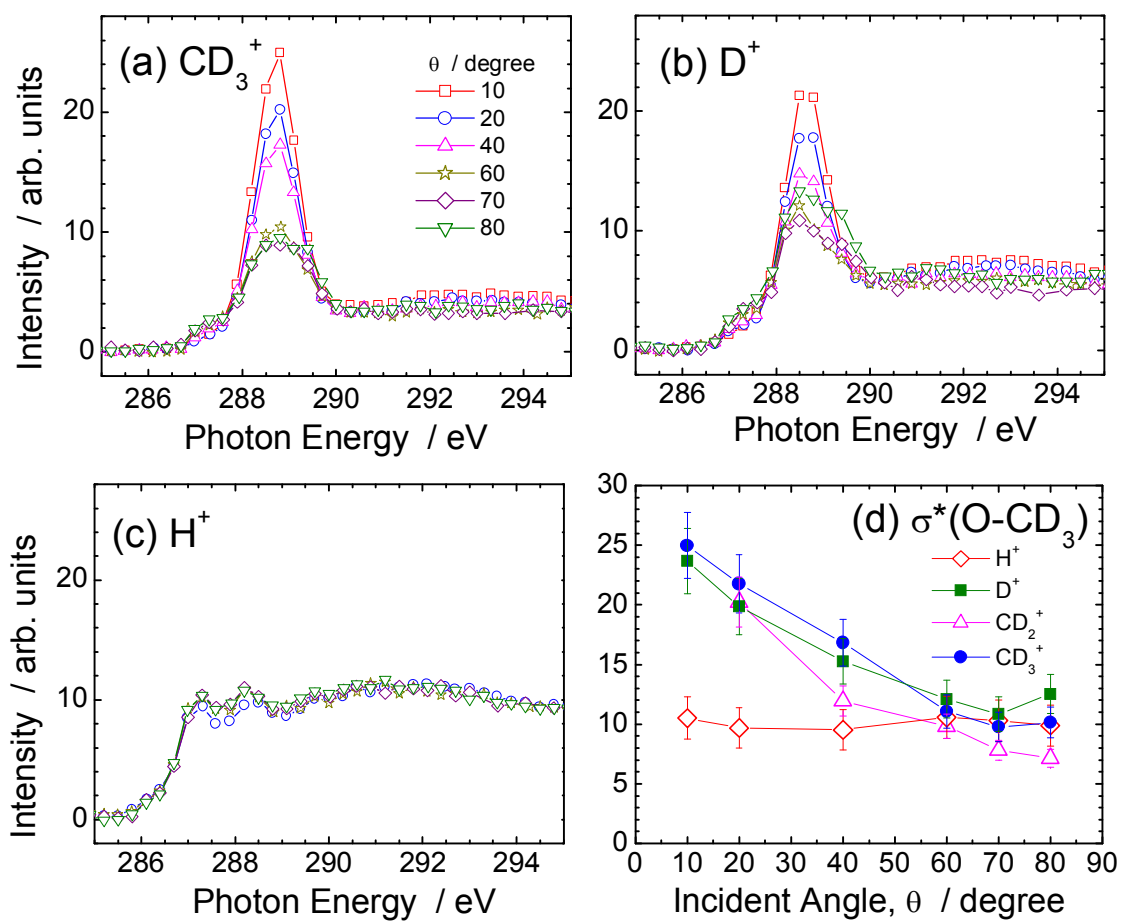


Figure 12. Normalized PIY spectra of (a) CD_3^+ , (b) D^+ and (c) H^+ ions measured for the MHTA- d_3 SAM in the C 1s region at different incident angles of SR. (d) Incident angle dependence of integrated PIY intensities of H^+ , D^+ , CD_2^+ and CD_3^+ ions for the net $\sigma^*(O-CD_3)$ excitation.

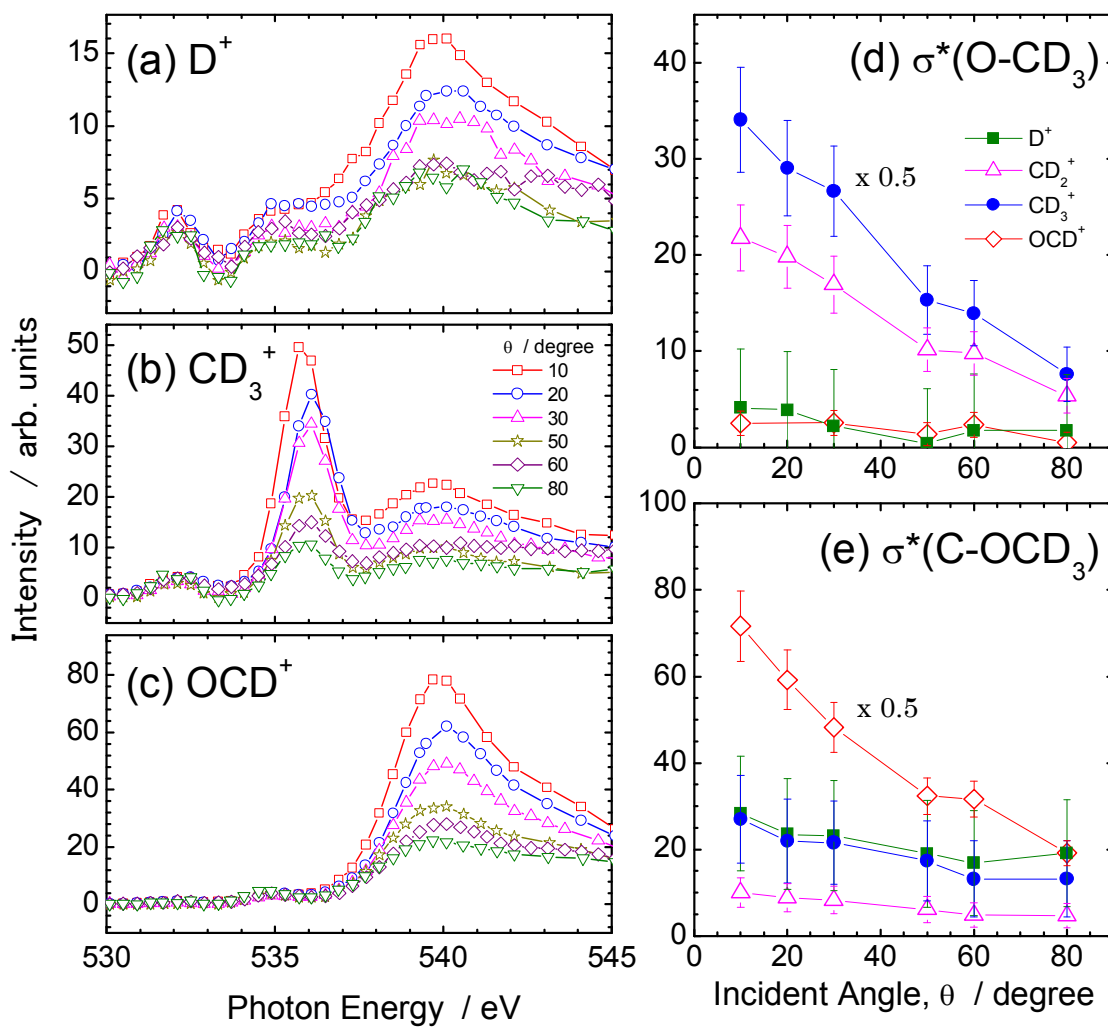


Figure 13. Normalized PIY spectra of (a) D^+ , (b) CD_3^+ and (c) OCD^+ ions measured for the MHDA- d_3 SAM in the O 1s region at different incident angles of SR. (e), (f) Incident angle dependence of integrated PIY intensities of D^+ , CD_2^+ , CD_3^+ and OCD^+ ions for the net $\sigma^*(O-CD_3)$ and $\sigma^*(C-OCD_3)$ excitations. Intensities of CD_3^+ in $\sigma^*(O-CD_3)$ and OCD^+ in $\sigma^*(C-OCD_3)$ are both multiplied by 0.5.

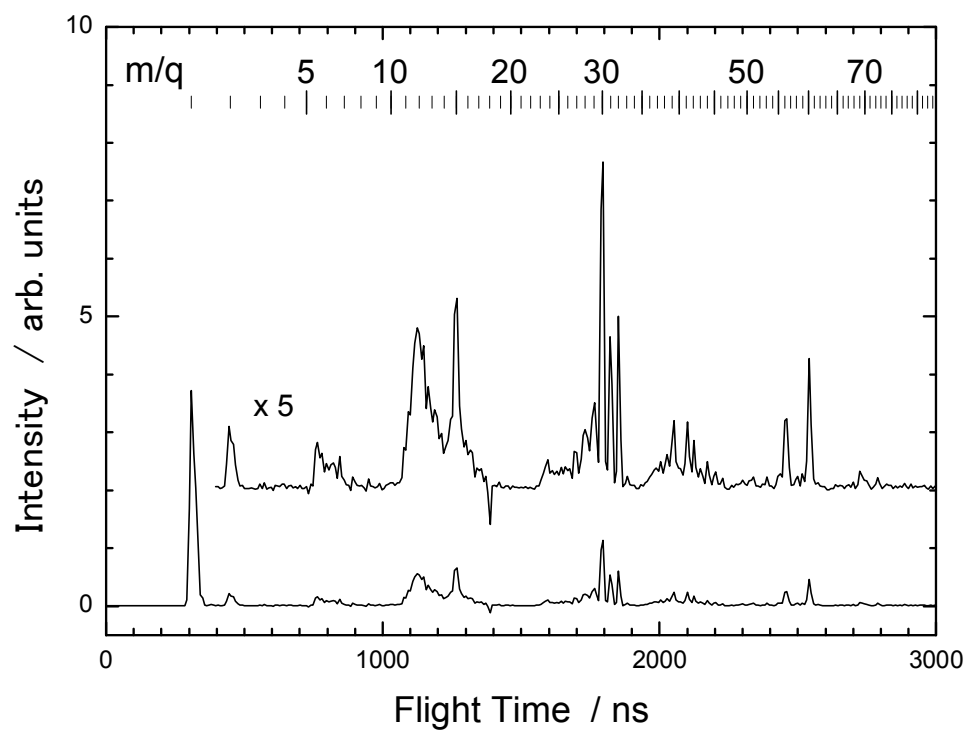


Figure 14. Typical TOF spectra of neutral photofragments desorbing from core-excited PMMA. Photon energy of SR is tuned to the $\sigma^*(\text{C}-\text{OCH}_3) \leftarrow \text{O } 1s(\text{OCH}_3)$ excitation.

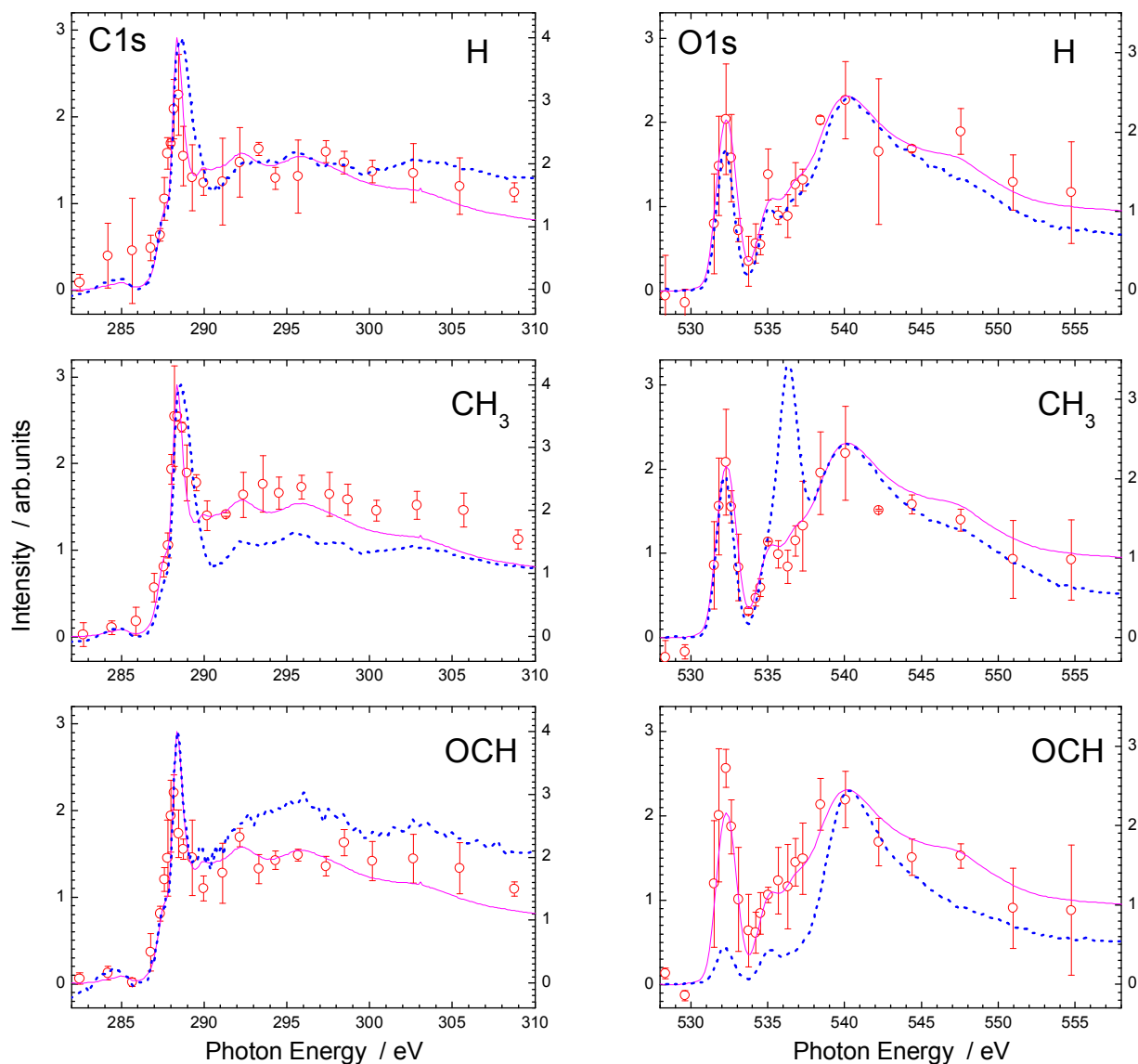


Figure 15. Plots of photodesorbing neutral fragments of H, CH₃ and OCH for the core-excited PMMA as a function of the photon energy. TEY (solid line) and corresponding PIY (dotted line) spectra are also drawn. Each PSD yield of neutral and ion is aligned to the corresponding TEY spectrum.